

1 **The gammaherpesvirus 68 viral cyclin facilitates reactivation by promoting**  
2 **latent gene expression.**

3 Brian F Niemeyer<sup>1</sup>, Joy E Gibson<sup>2</sup>, Jennifer N Berger<sup>1</sup>, Lauren M Oko<sup>1</sup>, Eva  
4 Medina<sup>1</sup>, Eric T Clambey<sup>3</sup>, Linda F van Dyk<sup>1</sup>

5  
6 <sup>1</sup>Immunology and Microbiology Department, University of Colorado Denver  
7 School of Medicine, Aurora, Colorado, USA, <sup>2</sup>Department of Pediatrics,  
8 University of Colorado School of Medicine, Aurora, Colorado, <sup>3</sup>Department of  
9 Anesthesiology, University of Colorado Anschutz Medical Campus, Aurora,  
10 Colorado

11 Address correspondence to: Linda F. van Dyk, University of Colorado School of  
12 Medicine, 12800 E. 19th Ave., MS8333, P.O. Box 6511, Aurora, CO, 80045.  
13 Phone: (303) 724-4207. Fax: (303) 724-4226. Email:  
14 Linda.VanDyk@ucdenver.edu

15 **Running Title:** viral cyclin is required for optimal gene expression

16 **Keywords:** gammaherpesvirus, LANA, reactivation, viral cyclin, gene expression

17

18 **Abstract**

19 Gammaherpesviruses establish life-long infections within their host and have  
20 been shown to be the causative agents of devastating malignancies. Chronic  
21 infection within the host is mediated through cycles of transcriptionally quiescent  
22 stages of latency with periods of reactivation into more active lytic and productive

23 infection. The mechanisms that regulate reactivation from latency remain poorly  
24 understood. Previously, we defined a critical role for the viral cyclin in promoting  
25 reactivation from latency. Disruption of the viral cyclin had no impact on the  
26 frequency of cells containing viral genome during latency, yet it remains unclear  
27 whether the viral cyclin influences latently infected cells in a qualitative manner.  
28 To define the impact of the viral cyclin on latent gene expression, we utilized a  
29 viral cyclin deficient variant expressing a LANA-beta-lactamase fusion protein  
30 (LANA:: $\beta$ la), to enumerate both the cellular distribution and frequency of latent  
31 gene expression. Disruption of the viral cyclin did not affect the cellular  
32 distribution of latently infected cells, but did result in a significant decrease in the  
33 frequency of cells that expressed LANA:: $\beta$ la across multiple tissues and in both  
34 immunocompetent and immunodeficient hosts. Strikingly, whereas the cyclin-  
35 deficient virus had a reactivation defect in bulk culture, sort purified cyclin-  
36 deficient LANA:: $\beta$ la expressing cells were fully capable of reactivation. These  
37 data emphasize that the  $\gamma$ HV68 latent reservoir is comprised of at least two  
38 distinct stages of infection characterized by differential latent gene expression,  
39 and that a primary function of the viral cyclin is to promote latent gene expression  
40 within infected cells in vivo.

#### 41 **AUTHOR SUMMARY**

42 Gammaherpesviruses are ubiquitous viruses with oncogenic potential that establish  
43 latency for the life of the host. These viruses can emerge from latency through  
44 reactivation, a process that is controlled by the immune system. Control of viral latency  
45 and reactivation is thought to be critical to prevent  $\gamma$ HV-associated disease. This study  
46 focuses on a virally-encoded cyclin that is required for reactivation from latency. By

47 characterizing how the viral cyclin influences latent infection in pure cell populations, we  
48 find that the viral cyclin has a vital role in promoting viral gene expression during latency.  
49 This work provides new insight into the function of a virally encoded cyclin in promoting  
50 reactivation from latency.

51

52

### 53 **Introduction**

54 Gammaherpesviruses ( $\gamma$ HV) are a group of lymphotropic viruses within  
55 the herpesviridae family, including the human pathogens Epstein-Barr virus  
56 (EBV) and Kaposi's sarcoma-associated herpesvirus (KSHV, HHV-8). Infection  
57 with these viruses is known to result in development of a wide range of  
58 malignancies including Burkitt's lymphoma, Kaposi's sarcoma, nasopharyngeal  
59 carcinoma, post-transplant lymphoproliferative disorders, and primary effusion  
60 lymphoma [1, 2]. The naturally occurring mouse gammaherpesvirus,  $\gamma$ HV68, is  
61 closely related to both EBV and KSHV, readily infects laboratory strains of mice,  
62 and provides insights into the complex processes of  $\gamma$ HV pathogenesis [3, 4].

63  $\gamma$ HV infection can be characterized by two distinct phases, lytic and  
64 latent infection. Lytic infection is a productive form of infection in which the entire  
65 suite of viral genes is expressed and the virus actively replicates its genome [5-  
66 7]. In this process, new virus is produced and the lytically infected cell dies.  
67 Alternatively, the virus may enter a latent state of infection, in which viral gene  
68 expression is mostly suppressed and the viral genome is maintained as an  
69 episome in the host nucleus [8].  $\gamma$ HV are able to switch from latent to lytic

70 infection through a process known as reactivation [9, 10]. These viruses are able  
71 to establish latent infection in many different cell types including dendritic cells,  
72 macrophages, and multiple B cell subsets (including memory B cells, plasma  
73 cells, B1-a cells, and B1-b B cells) [11-17]. Although several cell types support  
74 latent infection, the relative efficiency of these cell types to support reactivation  
75 remains unknown. Numerous studies suggest that a primary source of  
76 reactivating virus is plasma cells [14, 18-20]. Other studies indicate that in the  
77 peritoneal compartment, infected macrophages and/or B1 B cells are major cell  
78 types capable of reactivation [12, 13].

79           Many viral and host factors contribute to the control of latent infection  
80 and reactivation. KSHV and  $\gamma$ HV68 both encode a conserved viral cyclin (v-  
81 cyclin), which is homologous to host D-type cyclins [3, 21, 22]. Although EBV  
82 does not encode its own cyclin, it expresses viral genes that upregulate host  
83 cyclin D2, fulfilling a similar function to the KSHV and  $\gamma$ HV68 v-cyclin [23]. Like  
84 the host cyclins, the v-cyclin has the ability to interact with host cyclin-dependent  
85 kinases (CDKs) and promote cell cycle progression [24, 25]. Unlike conventional  
86 host cyclins, the v-cyclin is resistant to inhibition by CDK inhibitors (CKI) [26].  
87 Recent work by our group showed that one mechanism by which the v-cyclin  
88 promotes reactivation is by antagonizing the host CKI p18Ink4c, in a cell intrinsic  
89 manner [27, 28].

90           Although the v-cyclin is required for reactivation from latency, the  
91 underlying mechanisms by which it promotes reactivation have yet to be  
92 elucidated. Here, we studied how the v-cyclin may influence latent gene

93 expression in vivo, through the use of recombinant  $\gamma$ HV68 viruses that encode a  
94 fusion of the ORF73/LANA latency-associated gene with  $\beta$ -lactamase, a robust  
95 enzymatic reporter gene that can be used to identify individual virally-infected  
96 cells [28, 29], referred to as LANA:: $\beta$ la. By comparing wild-type and cyclin-  
97 deficient viruses, we were able to quantify the frequency and cellular distribution  
98 of LANA:: $\beta$ la gene expression during latency. These studies demonstrate that  
99 the v-cyclin has a critical role in promoting expression of LANA:: $\beta$ la at the single-  
100 cell level, with no discernable impact on the cellular distribution of infection.  
101 Further, we find that the v-cyclin is completely dispensable for reactivation, when  
102 reactivation efficiency is tested in LANA:: $\beta$ la expressing cells. The work detailed  
103 here serves to further our understanding of how the virus regulates reactivation.  
104 We also highlight an emerging trend in the field of virology where latency is not a  
105 uniform state of infection. Rather, some latently infected cells are poised for  
106 reactivation, while other infected cells appear to be refractory to reactivation.

## 107 **Results**

108 **A cycKO virus expressing a fusion between LANA and  $\beta$ -**  
109 **lactamase is equivalent to wild-type virus in LANA:: $\beta$ la expression during**  
110 **lytic infection, but deficient in reactivation.** The v-cyclin is required for  $\gamma$ HV68  
111 reactivation. Virus lacking v-cyclin, cycKO, is equivalent to wild-type virus in  
112 replication and establishment of latency, but is selectively defective in  
113 reactivation from latency [30, 31]. Given that some cell types may be more  
114 permissive to reactivation from latency than others, we proposed that the cycKO  
115 virus may be enriched in, or limited to, a “less permissive” cell type. To address

116 this, we made use of two previously described enzymatically marked viruses,  
117 WT. $\beta$ la and cycKO. $\beta$ la [28, 29]. These viruses both contain a fusion protein  
118 where  $\beta$ -lactamase is fused to the viral LANA (Fig 1A). This can be used to  
119 efficiently identify infected cells by flow cytometry using LANA:: $\beta$ la expression as  
120 a surrogate indicator of virus infection. Fusion of  $\beta$ -lactamase to LANA does not  
121 appear to alter viral replication, establishment of latency, or reactivation from  
122 latency [28, 29, 32]. To confirm this reporter system works equivalently for the  
123 WT. $\beta$ la and cycKO. $\beta$ la viruses, we measured the frequency and expression of  
124 LANA:: $\beta$ la after lytic infection of mouse 3T12 fibroblasts. 3T12 cells were infected  
125 at an MOI of 10 with WT (unmarked), WT. $\beta$ la, or cycKO. $\beta$ la virus. At 12 hours  
126 post infection (hpi), cells were collected, and stained for  $\beta$ -lactamase activity  
127 using CCF2-AM, a cell-permeable  $\beta$ -lactamase substrate [28, 29, 32]. CCF2-AM  
128 is readily taken up by living cells, causing them to fluoresce at 520nm. If  $\beta$ -  
129 lactamase is present, indicating viral LANA expression, it then cleaves the  
130 substrate causing the cells to gain fluorescence emission at 448 nm. As  
131 expected, WT. $\beta$ la and cycKO. $\beta$ la viruses resulted in comparable frequency and  
132 expression of LANA:: $\beta$ la ( $\beta$ la<sup>+</sup>) following in vitro infection (Fig 1B). We next  
133 confirmed that, as reported, the  $\beta$ -lactamase marker did not alter reactivation  
134 phenotypes of either WT or cycKO viruses. C57BL/6 (B6) mice were infected  
135 with  $1 \times 10^6$  PFU of either WT. $\beta$ la or cycKO. $\beta$ la virus via intraperitoneal injection  
136 (IP). At 42 days post infection (dpi), splenocytes and peritoneal cells were  
137 collected and subjected to limiting-dilution reactivation analysis on permissive  
138 mouse embryonic fibroblasts (MEFs) as previously described [12, 33]. Briefly,

139 latently infected splenocytes and peritoneal cells were plated on MEFs. If latent  
140 virus reactivates, the resulting virions infect and lyse the MEF monolayer. The  
141 number of latently infected cells can then be determined through nonlinear  
142 regression analysis. As previously established in comparison of WT and cycKO  
143 viruses in absence of the  $\beta$  lactamase fusion, the cycKO. $\beta$ la virus was severely  
144 defective in reactivation from both splenocytes and peritoneal cells (Fig 1C).  
145 Taken together, these data support the previous reports that fusion of  $\beta$ -  
146 lactamase to LANA does not alter the biology of these viruses [28, 29, 32].

147 **The cell composition of cycKO. $\beta$ la infected mice is not altered**  
148 **compared to WT. $\beta$ la infection.** To determine if the cycKO virus is preferentially  
149 enriched in a particular subset of cells, we infected (B6) mice with  $1 \times 10^6$  PFU of  
150 either WT. $\beta$ la or cycKO. $\beta$ la via IP injection. Splenocytes were harvested at 8 dpi  
151 and 16 dpi. Eight dpi is a time point within the acute phase of infection, while 16  
152 dpi corresponds to the establishment of latency after acute infection has been  
153 resolved [34, 35]. After collection, splenocytes were stained for LANA:: $\beta$ la, CD19,  
154 IgD, CD38, and CD44. These markers were used to identify B cells (CD19<sup>+</sup>),  
155 including germinal center B cells (CD19<sup>+</sup>, IgD<sup>-</sup>, CD38<sup>-</sup>) or activated B cells  
156 (CD19<sup>+</sup>, IgD<sup>-</sup>, CD44<sup>+</sup>). We chose to measure these populations because  
157 germinal center B cells represent an important population for  $\gamma$ HV68 to infect and  
158 seed memory B cells [36], the primary cell type harboring long-term latent virus,  
159 and activating B cells has been show to stimulate reactivation [37]. We  
160 determined the composition of infected cells by identifying cells expressing the  
161 viral LANA:: $\beta$ la fusion protein (Fig 2A). We quantified germinal center B cells and

162 activated B cells by sequentially gating on CD19<sup>+</sup>, IgD<sup>-</sup>, and CD38<sup>-</sup> or CD44<sup>+</sup>  
163 respectively (Fig 2B). We saw no significant differences in the expression of  
164 these markers on total or infected ( $\beta$ la<sup>+</sup>) splenocytes at 8 dpi during acute  
165 infection (Fig 2C) or at 16 dpi during latency (Fig 2D). In agreement with this,  
166 there were no differences between WT. $\beta$ la or cycKO. $\beta$ la virus in the frequency of  
167  $\beta$ la<sup>+</sup> cells that were total B cells, germinal center B cells, or activated B cells (Fig  
168 2E). Contrary to our initial prediction, these data suggest that although the  
169 cycKO. $\beta$ la virus is defective in reactivation there are no appreciable differences  
170 in the composition of the infected cells compared to WT. $\beta$ la virus. Thus, there  
171 must be another explanation for the reactivation defect observed in v-cyclin  
172 deficient viruses.

173 **CycKO. $\beta$ la virus infection results in deficient expression of viral**  
174 **LANA compared to WT. $\beta$ la.** Splenocytes, from mice infected as above, were  
175 collected at 8 and 16 dpi and analyzed by limiting-dilution nested PCR to  
176 measure the frequency of splenocytes harboring viral DNA [12, 33]. We found  
177 that there was a minor decrease in the number of cells harboring cycKO. $\beta$ la virus  
178 at 8 dpi but no significant difference in the number of cells containing  $\gamma$ HV68 DNA  
179 following infection at 16 dpi (Fig 3A). These data indicate that the reactivation  
180 defect in cycKO virus is not due to fewer cells becoming infected, consistent with  
181 previously published reports [28, 30]. However, when splenocytes were  
182 analyzed for the frequency of LANA:: $\beta$ la expressing cells, we found a significantly  
183 lower frequency of LANA:: $\beta$ la<sup>+</sup> cells in mice infected with cycKO. $\beta$ la (0.06%)  
184 compared to wild-type virus infected samples (0.21%) at 8 dpi. Further, this trend



185 continued into latency with 0.03% of splenocytes at 16 dpi that were LANA:: $\beta$ la<sup>+</sup>  
186 after WT. $\beta$ la infection compared to 0.008% of splenocytes after cycKO. $\beta$ la  
187 infection (Fig 3B). This difference in frequency corresponded to a decrease in the  
188 total number of LANA:: $\beta$ la<sup>+</sup> splenocytes per mouse after infection with the  
189 cycKO. $\beta$ la virus (Fig 3C). Considering an equivalent number of cells are viral  
190 DNA positive (Fig 3A), this indicates that there is a decrease in the proportion of  
191 infected cells that expressed LANA in the absence of v-cyclin. This decreased  
192 frequency of LANA:: $\beta$ la<sup>+</sup> cells that are B cells, germinal center B cells, or memory  
193 B cells translated into a sharp decline in the number of LANA:: $\beta$ la<sup>+</sup> cells in  
194 cycKO. $\beta$ la infected mice compared to WT. $\beta$ la infected mice across multiple  
195 subsets (Fig 3D). As WT. $\beta$ la and cycKO. $\beta$ la viruses had comparable  $\beta$ -lactamase  
196 expression during lytic infection of 3T12 cells (Fig 1B), these data indicate that  
197 the v-cyclin promotes the frequency of LANA expressing cells during latent  
198 infection in vivo.

199 **The defect in LANA expression with cycKO. $\beta$ la infection is**  
200 **observed regardless of the tissue type.** While we consistently observed a  
201 decrease in the frequency of cells expressing LANA:: $\beta$ la after cycKO. $\beta$ la  
202 infection, it remained possible that this was a tissue-specific phenotype. To  
203 address this possibility, mice were infected IP as described above and peritoneal  
204 cells were collected at 8 and 16 dpi, stained for  $\beta$ -lactamase, CD19, and CD5.  
205 CD19 was used to distinguish between non-B cells and B cells (CD19<sup>+</sup>) and CD5  
206 expression on CD19<sup>+</sup> cells was used to identify B1-a cells, which are known to  
207 harbor latent virus in the peritoneum (Fig 4A) [13, 28]. We saw no significant

208 difference in the cellular distribution of infection between WT and cycKO viruses  
209 (Fig 4B), but a profound decrease in the frequency of LANA:: $\beta$ la<sup>+</sup> cells in  
210 peritoneal cells harvested from cycKO. $\beta$ la infected mice (Fig 4C). There was a  
211 significantly lower frequency of LANA:: $\beta$ la<sup>+</sup> peritoneal cells after cycKO. $\beta$ la  
212 infection at both 8 and 16 dpi (Fig 4D). This indicates that the v-cyclin is required  
213 for optimal LANA expression in the peritoneum and the spleen, two dominant  
214 sites for latency. Finally, to determine whether this effect was dependent on route  
215 of infection, we measured the frequency of LANA:: $\beta$ la<sup>+</sup> cells in the lungs at 8  
216 days post-intranasal infection (Supplemental Fig 1). Again, mice infected with  
217 cycKO. $\beta$ la virus had a reduced frequency and number of LANA:: $\beta$ la<sup>+</sup> compared  
218 to WT. $\beta$ la infected mice. These data demonstrate that the v-cyclin is required for  
219 optimal LANA expression, regardless of tissue or route of infection.

220 **The v-cyclin promotes the frequency of LANA expressing cells in**  
221 **immunodeficient, CD8-deficient mice.** The v-cyclin is required for optimal  
222 reactivation across both immunocompetent and immunodeficient genetic  
223 backgrounds [30, 33, 38]. CD8-deficient (CD8<sup>-/-</sup>) mice, which lack CD8 T cells,  
224 have a significant increase in the number of latently infected cells relative to B6  
225 controls [39]. Despite the overall increase in the number of latently infected cells,  
226 the cycKO. $\beta$ la virus is still defective in reactivation in these mice [33]. We  
227 therefore tested whether the v-cyclin was required to promote LANA expression  
228 in CD8<sup>-/-</sup> mice.

229 CD8<sup>-/-</sup> mice were infected via IP inoculation with either WT. $\beta$ la or  
230 cycKO. $\beta$ la virus. Splenocytes were harvested at 16 dpi and stained for  $\beta$ -

231 lactamase activity, CD19 expression, and IgD and CD38 expression on CD19<sup>+</sup>  
232 cells. We found that, as with B6 mice, there were no differences in cellular  
233 distribution of LANA::βla<sup>+</sup> between WT and cycKO viruses (Fig 5A, 5C).  
234 Importantly, the defect in LANA::βla expression in cycKO infected splenocytes is  
235 still maintained, with a 5.6-fold decrease in the frequency of splenocytes that are  
236 βla<sup>+</sup> after cycKO.βla infection (0.0034%) compared to WT.βla infection (0.019%)  
237 (Fig 5B). We also analyzed peritoneal cell infection at 16 dpi. Peritoneal cells  
238 from mice infected as above were collected and stained for β-lactamase activity,  
239 CD19, B220, and CD5. The cycKO.βla defect was also present in the peritoneal  
240 compartment, with only 0.054% of peritoneal cells LANA::βla<sup>+</sup> in cycKO infected  
241 samples compared to 0.496% LANA::βla<sup>+</sup> cells after WT.βla infection (Fig 6A,  
242 6B). Interestingly, we detected a modest shift in the peritoneal composition of  
243 LANA::βla<sup>+</sup> cycKO.βla infected cells: 25% of cycKO.βla infected LANA::βla<sup>+</sup> cells  
244 were CD19<sup>+</sup> compared to 12% of WT.βla infected LANA::βla<sup>+</sup> cells (Fig 6C). This  
245 difference mirrors a change in the total frequency of CD19<sup>+</sup> cells in the  
246 peritoneum after cycKO.βla infection (Fig 6C). When analyzing the composition  
247 of infected B cells by B220 and CD5 expression, the LANA::βla<sup>+</sup> cells were found  
248 in B1-a, B1-b, and B2 cells, with a higher prevalence in B1 populations. Of  
249 WT.βla infected LANA::βla<sup>+</sup> cells: 4% were B2 cells, 5% were B1-a cells, and 8%  
250 were B1-b cells. Of the cycKO.βla infected LANA::βla<sup>+</sup> cells: 10% were B2 cells,  
251 8% were B1-a cells, and 10% were B1-b cells (Fig 6C). Interestingly, we have  
252 previously identified a similar trend in p18Ink4c deficient mice, a mouse strain in  
253 which there is an overall increase in reactivation [28], similar to the CD8<sup>-/-</sup> mice.

254 To determine LANA:: $\beta$ la gene expression independent of enzymatic  
255 activity, we isolated WT or cycKO infected peritoneal cells and measured both  $\beta$ -  
256 lactamase and LANA RNA by qRT-PCR (Fig 6D). Similar to analysis by  
257 enzymatic activity, these data demonstrate a difference in latent gene expression  
258 at the RNA level between WT and cycKO infected cells at 16 dpi. These data  
259 indicate that the v-cyclin is required for optimal LANA gene expression in multiple  
260 tissues and in both immunocompetent and immunodeficient hosts.

261

262 **The v-cyclin is dispensable for reactivation in LANA expressing**  
263 **cells.** The reduced frequency of LANA expressing cells after cycKO. $\beta$ la infection  
264 in both B6 and CD8<sup>-/-</sup> mice correlates with the reactivation defect of the  
265 cycKO. $\beta$ la virus observed in these mice. It has also been previously reported that  
266 sort purifying LANA:: $\beta$ la<sup>+</sup> cells can enrich for cells capable of reactivation [29].  
267 Based on these observations, we postulated that the defect in reactivation of  
268 cycKO viruses may be a direct consequence of the reduced frequency of LANA  
269 expressing cells. To this end, we used flow sorting to purify LANA:: $\beta$ la<sup>+</sup> cells from  
270 mice infected with either WT. $\beta$ la and cycKO. $\beta$ la virus and measured reactivation  
271 capacity ex vivo. Given the low frequency of  $\beta$ la<sup>+</sup> cells in healthy B6 mice (Fig  
272 3B, 4C, and 5A), we sorted LANA:: $\beta$ la<sup>+</sup> cells from CD8<sup>-/-</sup> mice. CD8<sup>-/-</sup> mice were  
273 infected with WT. $\beta$ la or cycKO. $\beta$ la virus via IP injection with peritoneal cells  
274 harvested at 16 dpi, stained for  $\beta$ -lactamase expression and FACS purified into  
275 either LANA:: $\beta$ la<sup>+</sup> or LANA:: $\beta$ la<sup>-</sup> populations (Fig 7A), followed by flow cytometric  
276 analysis of sort purity (Fig 7B). For each sort, we recovered ~25,000-100,000

277 WT. $\beta$ la infected LANA:: $\beta$ la<sup>+</sup> cells, ~21,000-24,000 cycKO. $\beta$ la infected LANA:: $\beta$ la<sup>+</sup>  
278 cells, and ~1.5-2x10<sup>6</sup> LANA:: $\beta$ la<sup>-</sup> cells for each virus. Bulk, LANA:: $\beta$ la<sup>+</sup>, and  
279 LANA:: $\beta$ la<sup>-</sup> cells were plated by serial dilution on MEF monolayers and assessed  
280 for reactivation 21 days post-plating. As expected, in the pre-sorted population  
281 the cycKO. $\beta$ la virus showed a reactivation defect relative to WT. $\beta$ la infected  
282 peritoneal cells (Fig 7C). Reactivation in the LANA:: $\beta$ la<sup>-</sup> population was extremely  
283 low. In contrast to the low frequencies of reactivation present in the LANA:: $\beta$ la<sup>-</sup>  
284 population, LANA:: $\beta$ la<sup>+</sup> cultures had much higher frequencies of reactivation (Fig  
285 7C). Notably, when the number of LANA expressing cells analyzed for  
286 reactivation was normalized between WT. $\beta$ la and cycKO. $\beta$ la infected samples,  
287 the cycKO. $\beta$ la had equivalent reactivation to WT. $\beta$ la virus (Fig 7C). These data  
288 directly demonstrate that LANA expressing cells are enriched in their ability to  
289 reactivate from latency, and provide direct evidence that a primary function of the  
290 v-cyclin is to promote the frequency of LANA expressing cells during latent  
291 infection in vivo. They further indicate that the defect in reactivation observed in  
292 bulk cultures from cycKO infected mice can be directly attributed to a reduced  
293 frequency of LANA expressing cells in the cycKO infected latent reservoir.

294

## 295 **Discussion**

296 The balance between latency and reactivation is of critical importance in  
297  $\gamma$ HV infection and disease progression. Chronic infection with  $\gamma$ HV through  
298 maintenance of latency and reactivation has long been associated with virus-  
299 induced malignancies [1]. Here, we find that a primary function of the v-cyclin is

300 to promote latent gene expression (i.e. LANA), to create a reactivation competent  
301 latent reservoir. Our findings suggest that  $\gamma$ HV68 latency is not a uniform state.  
302 Indeed, it appears that some latently infected cells are more prone to reactivation  
303 while others seem refractory. In the work presented here, we show that LANA  
304 expression is a strong correlate with reactivation capacity, while cells that fail to  
305 express LANA have limited reactivation potential (Fig 7C). Therefore, we propose  
306 a more comprehensive model of gammaherpesvirus reactivation where either the  
307 viral cyclin, or potentially host cyclins, promote reactivation by altering the state  
308 of the latently infected cell (Fig 8). In this specific instance, expression of v-cyclin  
309 increases the pool of LANA expressing latently infected cells, which are more  
310 permissive to reactivation from latency (Fig 8).

311 The notion that viral latency is a diverse and complex state of infection  
312 was originally defined in EBV infection, in which there are several distinct types  
313 of latency [40]. These diverse latency stages are distinguished by variable  
314 expression of viral genes in a manner that is mimicked with cyclin-deficient  
315  $\gamma$ HV68 infection. Further, different EBV latency programs are associated with  
316 specific clinical outcomes and pathologies [41, 42]. While our findings likely  
317 reflect a conserved feature of biology amongst gammaherpesvirus, similar trends  
318 can be observed in latent infection across virus families. For example, in HIV  
319 infection, virus persists within the host through latency in many cells types,  
320 including CD4 T cell subsets and myeloid cells [43, 44]. Since these reservoirs  
321 cannot be cleared by therapeutics or the host immune system, one potential  
322 strategy for eradication of the virus is to trigger reactivation, resulting in death of

323 the cell by the virus or the host immune system [45]. One barrier to this approach  
324 is the fact that distinct populations of latently infected cells appeared differentially  
325 responsive to reactivation stimuli [46].

326 One important question raised by our findings is how broadly the v-cyclin  
327 is required for latent gene expression: is this effect specific to LANA, or does it  
328 apply more broadly to additional viral genes (e.g. M2)? In terms of how the v-  
329 cyclin is regulating latent gene expression, it is possible that loss of v-cyclin is  
330 associated with a defect in epigenetic remodeling, resulting in broad repression  
331 of viral gene expression. While the v-cyclin promotes the frequency of LANA  
332 expressing cells, it is notable that the LANA expression during latency can occur  
333 independent of the v-cyclin. In our previous studies, we have identified two  
334 contexts in which reactivation can occur in a v-cyclin independent manner: i)  
335 genetic, or physiological, loss of p18Ink4c enables robust reactivation of  $\gamma$ HV68  
336 in cycKO infection [27, 28], and ii) host cyclin D3 is capable of fulfilling the role of  
337 v-cyclin in driving reactivation in a cycKO background, albeit with a decreased  
338 efficiency [47]. Based on these observations, it is possible that cycKO infected  
339 cells with LANA expression may reflect cells with either increased cellular D type  
340 cyclin expression and/or decreased p18Ink4c expression, allowing both LANA  
341 expression and reactivation. Although our data emphasize that the v-cyclin  
342 promotes LANA expression and that LANA expressing cells are reactivation  
343 competent, it remains to be tested whether the v-cyclin supports additional  
344 features for optimal reactivation capacity.

345           The work described here documents a critical link between v-cyclin and  
346 viral LANA expression in reactivation from latency. Further, our findings strongly  
347 suggest that the latently infected reservoir is diverse in gene expression and  
348 reactivation capacity. These data identify a v-cyclin/LANA axis that is critical for  
349 reactivation from latency and emphasize that efforts to manipulate this axis may  
350 require a combinatorial approach that targets both v-cyclin dependent and  
351 independent processes to effectively disrupt the latent reservoir.

352

### 353 **Methods and Materials**

354           **Cell lines and viruses:** 3T12 mouse fibroblast cells (ATCC CCL-164)  
355 were cultured in 5% FBS/DMEM with 20 units of penicillin and 20  $\mu$ g of  
356 streptomycin per mL and 4 mM L-glutamine. MEFs were isolated as described  
357 and cultured in 10% FBS/DMEM with 20 units of penicillin per mL, 20  $\mu$ g of  
358 streptomycin per mL, 4 mM L-glutamine, and fungizone at 250 ng/mL [48].  
359 Generation of the WT. $\beta$ 1a and cycKO. $\beta$ 1a viruses has been previously described  
360 [28, 29, 32].

361           **Mice.** C57BL/6 (B6) mice were obtained from the Jackson Laboratory  
362 (Stock # 000664). CD8 $\alpha$ <sup>-/-</sup> mice on the B6 background (CD8<sup>-/-</sup>) were obtained  
363 from the Jackson Laboratory (Stock # 002665) and have been previously  
364 described [39]. CD8<sup>-/-</sup> mice were bred in house at the University of Colorado  
365 Denver Anschutz Medical Campus in accordance with University regulations and  
366 Institutional Animal Care and Use Committee.



367           **Flow cytometry analysis:** Splens were collected and splenocytes were  
368 isolated in a single cell suspension after being passed through a 100 micron  
369 filter. Splenocytes were then subjected to red blood cell lysis by treatment with  
370 red blood cell lysis buffer (Sigma # R7757) per manufacturer's recommendation.  
371 Peritoneal cells were collected with 10 mLs of cold 1% FBS DMEM.  $\beta$ -lactamase  
372 activity was detected using the LiveBLazer FRET-BG/Loading Kit with CCF2-AM  
373 (ThermoFischer Scientific # K1025) as previously described [17, 29, 32]. Cell  
374 surface antibodies used were CD19-AlexaFluor 700 (clone eBio1D3, eBioscience  
375 # 56-0193-81), CD38-APC (clone 90,eBiosciences #17-0382-81), IgD-APC-Cy7  
376 (clone 11-26c.2a, Biolegend # 405716), and CD5-APC (clone 53-7.3,  
377 eBioscience # 17-0051-81). Fc blocking antibody 24G2 was used in staining to  
378 prevent antibody binding to cellular Fc receptors.

379           **Limiting-dilution analysis:** Mice were inoculated with either WT. $\beta$ la or  
380 cycKO. $\beta$ la at  $1 \times 10^6$  PFU/mouse via IP injection. After 8 and 16 days, splenocytes  
381 and peritoneal cells were collected as above and analyzed by either flow  
382 cytometry or plated for reactivation or PCR analysis. By Poisson distribution, the  
383 number of cells plated corresponding to 63.2% of the wells positive is the  
384 frequency at which there is at least one reactivating or genome positive cell,  
385 respectively.

386           *Reactivation analysis.* Cells were subjected to serial limiting dilution  
387 analysis, and plated on highly permissive MEF monolayers for quantification of  
388 virus cytopathic effect as previously described [12, 33]. To control for any

389 preformed virus, mechanically disrupted peritoneal cells were plated in parallel;  
390 no monolayer disruption was observed in disrupted cells.

391 *LD-PCR analysis.* Cell dilutions were subjected to in-plate DNA isolation  
392 and nested-PCR for single copy sensitivity detection of viral gene 50 DNA, with  
393 plasmid sensitivity controls included on each plate, as previously described [12,  
394 33].

395 **Quantitative-PCR analysis:** CD8<sup>-/-</sup> mice were infected with  $1 \times 10^6$  PFU  
396 of either WT. $\beta$ la (n=3) or cycKO. $\beta$ la (n=3) virus or mock infected (n=2) via IP  
397 injection. At 16 dpi, peritoneal cells from individual mice were harvested from  
398 each mouse, pelleted at 1,000xg for 10 min, resuspended in RLT buffer  
399 containing  $\beta$ -mercaptoethanol and then frozen at -80°C. Cells were then thawed  
400 and homogenized via Qiashredder columns and RNA was isolated using the  
401 RNeasy Micro Kit. DNA was removed from the samples by treating with Turbo  
402 DNase as per the manufacturer's recommendations (ThermoFisher). cDNA was  
403 synthesized using Superscript II Reverse Transcriptase (ThermoFisher). Primers  
404 for SYBR Green qPCR were designed using Primer3. Primers used were: LANA  
405 Forward 5'-ATCAGGGAATGCGAAGACAC, LANA Reverse 5'-  
406 GTGCCTGGTACCAAGGGTAA,  $\beta$ -lactamase Forward 5'-  
407 GCTATGTGGCGCGGTATTAT,  $\beta$ -lactamase Reverse 5'-  
408 AAGTTGGCCGAGTGTTATC. iQ SYBR Green Supermix was used for the  
409 qPCR reactions (Bio-Rad) and qPCR was performed with technical triplicates  
410 from the peritoneal cell cDNA of each mouse, and run on the QuantStudio 7 Flex  
411 instrument.

412           **FACS sorted reactivation:** CD8<sup>-/-</sup> mice were infected with  $1 \times 10^6$  PFU of  
413 either WT. $\beta$ la or cycKO. $\beta$ la virus via IP injection. At 16 dpi, peritoneal cells were  
414 collected and combined for each virus group. For each virus group,  $1 \times 10^6$  cells  
415 were set aside as “pre-sorted” cells. The remaining cells were stained for  $\beta$ -  
416 lactamase then washed and resuspended in 2% FBS in PBS. These cells were  
417 then sorted by the Clinical Immunology Flow Core with the University of Colorado  
418 Anschutz Medical Campus. Cells were gated as single cells and then sorted into  
419  $\beta$ la<sup>+</sup> or  $\beta$ la<sup>-</sup> populations. A small number of LANA:: $\beta$ la<sup>+</sup> WT. $\beta$ la infected cells were  
420 tested for purity after the sort had concluded. The purity of the LANA:: $\beta$ la<sup>+</sup> cells  
421 was measured in the WT. $\beta$ la infected samples and found to be 97.3% pure . A  
422 corresponding purity check was not performed for the cycKO. $\beta$ la infected  
423 samples due to a lower total number of cells recovered. Pre-sorted, LANA:: $\beta$ la<sup>+</sup>,  
424 or LANA:: $\beta$ la<sup>-</sup> cells were diluted into 10% FBS in DMEM and plated onto  
425 permissive MEFs in a limiting-dilution fashion as previously described [12, 33].  
426 Pre-sorted and LANA:: $\beta$ la<sup>-</sup> cells were plated at starting concentrations of  $2 \times 10^4$   
427 cells per well while LANA:: $\beta$ la<sup>+</sup> cells were plated at a starting concentration of 100  
428 cells per well. Three weeks after plating cells, reactivation was measured by  
429 observation of cytopathic effect on the MEF cells.

430           **Statistical analysis and software:** Flow cytometric analysis was  
431 performed using FlowJo V.10.0.8r1. Graphs were generated and statistical  
432 analysis were performed using GraphPad Prism 7.0a. Limiting-dilution curves  
433 were created by performing a non-linear regression, log(agonist) vs. response-  
434 using the “EC anything” regression equation where F was set to 63.2, with top

435 and bottom of the curves constrained to 100 and 0 respectively. Comparisons of  
436 the LogECF were used to determine statistical significance. Unpaired student t-  
437 tests were performed as mentioned. Quantitative-PCR data was analyzed using  
438 the Pfaffl method [49] and graphed using GraphPad Prism 7.

439

440

- 441 1. Jha HC, Banerjee S, Robertson ES. The Role of Gammaherpesviruses in Cancer  
442 Pathogenesis. *Pathogens*. 2016;5(1). Epub 2016/02/11. doi:  
443 10.3390/pathogens5010018. PubMed PMID: 26861404; PubMed Central PMCID:  
444 PMC4810139.
- 445 2. Elgui de Oliveira D. DNA viruses in human cancer: an integrated overview on  
446 fundamental mechanisms of viral carcinogenesis. *Cancer Lett*. 2007;247(2):182-96.  
447 Epub 2006/07/04. doi: 10.1016/j.canlet.2006.05.010. PubMed PMID: 16814460.
- 448 3. Virgin HW, Latreille P, Wamsley P, Hallsworth K, Weck KE, Dal Canto AJ, et  
449 al. Complete sequence and genomic analysis of murine gammaherpesvirus 68. *J*  
450 *Virool*. 1997;71(8):5894-904. Epub 1997/08/01. PubMed PMID: 9223479; PubMed  
451 Central PMCID: PMC191845.
- 452 4. Speck SH, Virgin HW. Host and viral genetics of chronic infection: a mouse  
453 model of gamma-herpesvirus pathogenesis. *Curr Opin Microbiol*. 1999;2(4):403-9.  
454 Epub 1999/08/25. PubMed PMID: 10458986.
- 455 5. Cai Q, Verma SC, Lu J, Robertson ES. Molecular biology of Kaposi's sarcoma-  
456 associated herpesvirus and related oncogenesis. *Adv Virus Res*. 2010;78:87-142.  
457 Epub 2010/11/03. doi: 10.1016/B978-0-12-385032-4.00003-3. PubMed PMID:  
458 21040832; PubMed Central PMCID: PMC3142360.
- 459 6. Speck SH, Ganem D. Viral latency and its regulation: lessons from the gamma-  
460 herpesviruses. *Cell Host Microbe*. 2010;8(1):100-15. Epub 2010/07/20. doi:  
461 10.1016/j.chom.2010.06.014. PubMed PMID: 20638646; PubMed Central PMCID:  
462 PMC2914632.
- 463 7. Brown HJ, Song MJ, Deng H, Wu TT, Cheng G, Sun R. NF-kappaB inhibits  
464 gammaherpesvirus lytic replication. *J Virool*. 2003;77(15):8532-40. Epub  
465 2003/07/15. PubMed PMID: 12857922; PubMed Central PMCID: PMC165238.
- 466 8. Lieberman PM, Hu J, Renne R. Maintenance and replication during latency. In:  
467 Arvin A, Campadelli-Fiume G, Mocarski E, Moore PS, Roizman B, Whitley R, et al.,  
468 editors. *Human Herpesviruses: Biology, Therapy, and Immunoprophylaxis*.  
469 Cambridge 2007.
- 470 9. Grinde B. Herpesviruses: latency and reactivation - viral strategies and host  
471 response. *J Oral Microbiol*. 2013;5. Epub 2013/10/30. doi: 10.3402/jom.v5i0.22766.  
472 PubMed PMID: 24167660; PubMed Central PMCID: PMC3809354.

- 473 10. Murata T, Tsurumi T. Switching of EBV cycles between latent and lytic states.  
474 *Rev Med Virol.* 2014;24(3):142-53. Epub 2013/12/18. doi: 10.1002/rmv.1780.  
475 PubMed PMID: 24339346.
- 476 11. Willer DO, Speck SH. Long-term latent murine Gammaherpesvirus 68  
477 infection is preferentially found within the surface immunoglobulin D-negative  
478 subset of splenic B cells in vivo. *J Virol.* 2003;77(15):8310-21. Epub 2003/07/15.  
479 PubMed PMID: 12857900; PubMed Central PMCID: PMCPMC165249.
- 480 12. Weck KE, Kim SS, Virgin HI, Speck SH. Macrophages are the major reservoir  
481 of latent murine gammaherpesvirus 68 in peritoneal cells. *J Virol.* 1999;73(4):3273-  
482 83. Epub 1999/03/12. PubMed PMID: 10074181; PubMed Central PMCID:  
483 PMCPMC104091.
- 484 13. Rekow MM, Darrah EJ, Mboko WP, Lange PT, Tarakanova VL.  
485 Gammaherpesvirus targets peritoneal B-1 B cells for long-term latency. *Virology.*  
486 2016;492:140-4. Epub 2016/03/06. doi: 10.1016/j.virol.2016.02.022. PubMed  
487 PMID: 26945150; PubMed Central PMCID: PMCPMC4826794.
- 488 14. Liang X, Collins CM, Mendel JB, Iwakoshi NN, Speck SH. Gammaherpesvirus-  
489 driven plasma cell differentiation regulates virus reactivation from latently infected  
490 B lymphocytes. *PLoS Pathog.* 2009;5(11):e1000677. Epub 2009/12/04. doi:  
491 10.1371/journal.ppat.1000677. PubMed PMID: 19956661; PubMed Central PMCID:  
492 PMCPMC2777334.
- 493 15. Flano E, Husain SM, Sample JT, Woodland DL, Blackman MA. Latent murine  
494 gamma-herpesvirus infection is established in activated B cells, dendritic cells, and  
495 macrophages. *J Immunol.* 2000;165(2):1074-81. Epub 2000/07/06. PubMed PMID:  
496 10878386.
- 497 16. Collins CM, Speck SH. Tracking murine gammaherpesvirus 68 infection of  
498 germinal center B cells in vivo. *PLoS One.* 2012;7(3):e33230. Epub 2012/03/20. doi:  
499 10.1371/journal.pone.0033230. PubMed PMID: 22427999; PubMed Central PMCID:  
500 PMCPMC3302828.
- 501 17. Coleman CB, Nealy MS, Tibbetts SA. Immature and transitional B cells are  
502 latency reservoirs for a gammaherpesvirus. *J Virol.* 2010;84(24):13045-52. Epub  
503 2010/10/12. doi: 10.1128/JVI.01455-10. PubMed PMID: 20926565; PubMed  
504 Central PMCID: PMCPMC3004345.
- 505 18. Wilson SJ, Tsao EH, Webb BL, Ye H, Dalton-Griffin L, Tsantoulas C, et al. X box  
506 binding protein XBP-1s transactivates the Kaposi's sarcoma-associated herpesvirus  
507 (KSHV) ORF50 promoter, linking plasma cell differentiation to KSHV reactivation  
508 from latency. *J Virol.* 2007;81(24):13578-86. Epub 2007/10/12. doi:  
509 10.1128/JVI.01663-07. PubMed PMID: 17928342; PubMed Central PMCID:  
510 PMCPMC2168861.
- 511 19. Sun CC, Thorley-Lawson DA. Plasma cell-specific transcription factor XBP-1s  
512 binds to and transactivates the Epstein-Barr virus BZLF1 promoter. *J Virol.*  
513 2007;81(24):13566-77. Epub 2007/09/28. doi: 10.1128/JVI.01055-07. PubMed  
514 PMID: 17898050; PubMed Central PMCID: PMCPMC2168822.
- 515 20. Laichalk LL, Thorley-Lawson DA. Terminal differentiation into plasma cells  
516 initiates the replicative cycle of Epstein-Barr virus in vivo. *J Virol.* 2005;79(2):1296-  
517 307. Epub 2004/12/23. doi: 10.1128/JVI.79.2.1296-1307.2005. PubMed PMID:  
518 15613356; PubMed Central PMCID: PMCPMC538585.

- 519 21. Li M, Lee H, Yoon DW, Albrecht JC, Fleckenstein B, Neipel F, et al. Kaposi's  
520 sarcoma-associated herpesvirus encodes a functional cyclin. *J Virol.*  
521 1997;71(3):1984-91. Epub 1997/03/01. PubMed PMID: 9032330; PubMed Central  
522 PMCID: PMCPMC191282.
- 523 22. Chang Y, Moore PS, Talbot SJ, Boshoff CH, Zarkowska T, Godden K, et al.  
524 Cyclin encoded by KS herpesvirus. *Nature.* 1996;382(6590):410. Epub 1996/08/01.  
525 doi: 10.1038/382410a0. PubMed PMID: 8684480.
- 526 23. Arvanitakis L, Yaseen N, Sharma S. Latent membrane protein-1 induces cyclin  
527 D2 expression, pRb hyperphosphorylation, and loss of TGF-beta 1-mediated growth  
528 inhibition in EBV-positive B cells. *J Immunol.* 1995;155(3):1047-56. Epub  
529 1995/08/01. PubMed PMID: 7636179.
- 530 24. van Dyk LF, Hess JL, Katz JD, Jacoby M, Speck SH, Virgin HI. The murine  
531 gammaherpesvirus 68 v-cyclin gene is an oncogene that promotes cell cycle  
532 progression in primary lymphocytes. *J Virol.* 1999;73(6):5110-22. Epub  
533 1999/05/11. PubMed PMID: 10233974; PubMed Central PMCID: PMCPMC112556.
- 534 25. Upton JW, van Dyk LF, Speck SH. Characterization of murine  
535 gammaherpesvirus 68 v-cyclin interactions with cellular cdks. *Virology.*  
536 2005;341(2):271-83. Epub 2005/08/17. doi: 10.1016/j.virol.2005.07.014. PubMed  
537 PMID: 16102793.
- 538 26. Swanton C, Mann DJ, Fleckenstein B, Neipel F, Peters G, Jones N. Herpes viral  
539 cyclin/Cdk6 complexes evade inhibition by CDK inhibitor proteins. *Nature.*  
540 1997;390(6656):184-7. Epub 1997/11/21. doi: 10.1038/36606. PubMed PMID:  
541 9367157.
- 542 27. Williams LM, Niemeyer BF, Franklin DS, Clambey ET, van Dyk LF. A  
543 Conserved Gammaherpesvirus Cyclin Specifically Bypasses Host p18(INK4c) To  
544 Promote Reactivation from Latency. *J Virol.* 2015;89(21):10821-31. Epub  
545 2015/08/21. doi: 10.1128/JVI.00891-15. PubMed PMID: 26292318; PubMed  
546 Central PMCID: PMCPMC4621100.
- 547 28. Niemeyer BF, Oko LM, Medina EM, Oldenburg DG, White DW, Cool CD, et al.  
548 Host Tumor Suppressor p18(INK4c) Functions as a Potent Cell-Intrinsic Inhibitor of  
549 Murine Gammaherpesvirus 68 Reactivation and Pathogenesis. *J Virol.* 2018;92(6).  
550 Epub 2018/01/05. doi: 10.1128/JVI.01604-17. PubMed PMID: 29298882; PubMed  
551 Central PMCID: PMCPMC5827403.
- 552 29. Nealy MS, Coleman CB, Li H, Tibbetts SA. Use of a virus-encoded enzymatic  
553 marker reveals that a stable fraction of memory B cells expresses latency-associated  
554 nuclear antigen throughout chronic gammaherpesvirus infection. *J Virol.*  
555 2010;84(15):7523-34. Epub 2010/05/21. doi: 10.1128/JVI.02572-09. PubMed  
556 PMID: 20484501; PubMed Central PMCID: PMCPMC2897616.
- 557 30. van Dyk LF, Virgin HWt, Speck SH. The murine gammaherpesvirus 68 v-  
558 cyclin is a critical regulator of reactivation from latency. *J Virol.* 2000;74(16):7451-  
559 61. Epub 2000/07/25. PubMed PMID: 10906198; PubMed Central PMCID:  
560 PMCPMC112265.
- 561 31. Hoge AT, Hendrickson SB, Burns WH. Murine gammaherpesvirus 68 cyclin D  
562 homologue is required for efficient reactivation from latency. *J Virol.*  
563 2000;74(15):7016-23. Epub 2000/07/11. PubMed PMID: 10888640; PubMed  
564 Central PMCID: PMCPMC112218.

- 565 32. Diebel KW, Oko LM, Medina EM, Niemeyer BF, Warren CJ, Claypool DJ, et al.  
566 Gammaherpesvirus small noncoding RNAs are bifunctional elements that regulate  
567 infection and contribute to virulence in vivo. *MBio*. 2015;6(1):e01670-14. Epub  
568 2015/02/19. doi: 10.1128/mBio.01670-14. PubMed PMID: 25691585; PubMed  
569 Central PMCID: PMC4337559.
- 570 33. van Dyk LF, Virgin HWt, Speck SH. Maintenance of gammaherpesvirus  
571 latency requires viral cyclin in the absence of B lymphocytes. *J Virol*.  
572 2003;77(9):5118-26. Epub 2003/04/15. PubMed PMID: 12692214; PubMed Central  
573 PMCID: PMC153990.
- 574 34. Tibbetts SA, Loh J, Van Berkel V, McClellan JS, Jacoby MA, Kapadia SB, et al.  
575 Establishment and maintenance of gammaherpesvirus latency are independent of  
576 infective dose and route of infection. *J Virol*. 2003;77(13):7696-701. Epub  
577 2003/06/14. PubMed PMID: 12805472; PubMed Central PMCID: PMC164792.
- 578 35. Sunil-Chandra NP, Efstathiou S, Nash AA. Murine gammaherpesvirus 68  
579 establishes a latent infection in mouse B lymphocytes in vivo. *J Gen Virol*. 1992;73 ( Pt 12):3275-9. Epub 1992/12/01. doi: 10.1099/0022-1317-73-12-3275. PubMed  
580 PMID: 1469366.
- 582 36. Herskowitz JH, Jacoby MA, Speck SH. The murine gammaherpesvirus 68 M2  
583 gene is required for efficient reactivation from latently infected B cells. *J Virol*.  
584 2005;79(4):2261-73. Epub 2005/02/01. doi: 10.1128/JVI.79.4.2261-2273.2005.  
585 PubMed PMID: 15681428; PubMed Central PMCID: PMC546582.
- 586 37. Moser JM, Upton JW, Gray KS, Speck SH. Ex vivo stimulation of B cells latently  
587 infected with gammaherpesvirus 68 triggers reactivation from latency. *J Virol*.  
588 2005;79(8):5227-31. Epub 2005/03/30. doi: 10.1128/JVI.79.8.5227-5231.2005.  
589 PubMed PMID: 15795307; PubMed Central PMCID: PMC1069562.
- 590 38. Gangappa S, van Dyk LF, Jewett TJ, Speck SH, Virgin HWt. Identification of the  
591 in vivo role of a viral bcl-2. *J Exp Med*. 2002;195(7):931-40. Epub 2002/04/03.  
592 PubMed PMID: 11927636; PubMed Central PMCID: PMC2193719.
- 593 39. Tibbetts SA, van Dyk LF, Speck SH, Virgin HWt. Immune control of the  
594 number and reactivation phenotype of cells latently infected with a  
595 gammaherpesvirus. *J Virol*. 2002;76(14):7125-32. Epub 2002/06/20. PubMed  
596 PMID: 12072512; PubMed Central PMCID: PMC136321.
- 597 40. Lieberman PM. Keeping it quiet: chromatin control of gammaherpesvirus  
598 latency. *Nat Rev Microbiol*. 2013;11(12):863-75. Epub 2013/11/07. doi:  
599 10.1038/nrmicro3135. PubMed PMID: 24192651; PubMed Central PMCID:  
600 PMC4544771.
- 601 41. Niedobitek G, Meru N, Delecluse HJ. Epstein-Barr virus infection and human  
602 malignancies. *Int J Exp Pathol*. 2001;82(3):149-70. Epub 2001/08/08. PubMed  
603 PMID: 11488990; PubMed Central PMCID: PMC2517709.
- 604 42. Hussain T, Mulherkar R. Lymphoblastoid Cell lines: a Continuous in Vitro  
605 Source of Cells to Study Carcinogen Sensitivity and DNA Repair. *Int J Mol Cell Med*.  
606 2012;1(2):75-87. Epub 2012/04/01. PubMed PMID: 24551762; PubMed Central  
607 PMCID: PMC3920499.
- 608 43. Siliciano RF, Greene WC. HIV latency. *Cold Spring Harb Perspect Med*.  
609 2011;1(1):a007096. Epub 2012/01/10. doi: 10.1101/cshperspect.a007096.  
610 PubMed PMID: 22229121; PubMed Central PMCID: PMC3234450.

- 611 44. Lee GQ, Lichterfeld M. Diversity of HIV-1 reservoirs in CD4+ T-cell  
612 subpopulations. *Curr Opin HIV AIDS*. 2016;11(4):383-7. Epub 2016/03/30. doi:  
613 10.1097/COH.0000000000000281. PubMed PMID: 27023286; PubMed Central  
614 PMCID: PMCPMC4915926.
- 615 45. Datta PK, Kaminski R, Hu W, Pirrone V, Sullivan NT, Nonnemacher MR, et al.  
616 HIV-1 Latency and Eradication: Past, Present and Future. *Curr HIV Res*.  
617 2016;14(5):431-41. Epub 2016/03/25. PubMed PMID: 27009094; PubMed Central  
618 PMCID: PMCPMC5157928.
- 619 46. Baxter AE, Niessl J, Fromentin R, Richard J, Porichis F, Charlebois R, et al.  
620 Single-Cell Characterization of Viral Translation-Competent Reservoirs in HIV-  
621 Infected Individuals. *Cell Host Microbe*. 2016;20(3):368-80. Epub 2016/08/23. doi:  
622 10.1016/j.chom.2016.07.015. PubMed PMID: 27545045; PubMed Central PMCID:  
623 PMCPMC5025389.
- 624 47. Lee KS, Suarez AL, Claypool DJ, Armstrong TK, Buckingham EM, van Dyk LF.  
625 Viral cyclins mediate separate phases of infection by integrating functions of distinct  
626 mammalian cyclins. *PLoS Pathog*. 2012;8(2):e1002496. Epub 2012/02/10. doi:  
627 10.1371/journal.ppat.1002496. PubMed PMID: 22319441; PubMed Central PMCID:  
628 PMCPMC3271081.
- 629 48. Weck KE, Barkon ML, Yoo LI, Speck SH, Virgin HI. Mature B cells are required  
630 for acute splenic infection, but not for establishment of latency, by murine  
631 gammaherpesvirus 68. *J Virol*. 1996;70(10):6775-80. Epub 1996/10/01. PubMed  
632 PMID: 8794315; PubMed Central PMCID: PMCPMC190721.
- 633 49. Pfaffl MW. A new mathematical model for relative quantification in real-time  
634 RT-PCR. *Nucleic Acids Res*. 2001;29(9):e45. Epub 2001/05/09. PubMed PMID:  
635 11328886; PubMed Central PMCID: PMCPMC55695.  
636



**Figure 1. Characterization of the cyclin-deficient virus expressing a LANA  $\beta$ -lactamase gene fusion.** (A) Schematic of wild-type virus (top), the cyclin deficient virus (second), the wild-type  $\beta$ -lactamase marked virus (third), and the cyclin deficient  $\beta$ -lactamase marked virus (bottom). Viruses described as in van Dyk 2000 and Niemeyer 2018. (B) Identification of infected cells by flow cytometry using  $\beta$ -lactamase ( $\beta$ la). 3T12 cells were infected with either wild-type unmarked  $\gamma$ HV68, WT. $\beta$ la, or cycKO. $\beta$ la at an MOI of 10 pfu/cell. Cells were harvested at 12 hpi and infected cells were identified by  $\beta$ -lactamase activity. LANA:: $\beta$ la<sup>+</sup> cells are contained within the upper right polygonal gate. Average LANA:: $\beta$ la<sup>+</sup> frequencies are indicated +/- SEM n=2. (C) B6 mice were infected via IP infection with WT. $\beta$ la (black) or cycKO. $\beta$ la (red) viruses. At 42 dpi splenocytes (left panel) and peritoneal cells (right panel) from infected mice were plated on MEFs in a limiting-dilution fashion. Comparison of reactivation from infected cells were pooled for reactivation analysis. For each virus group 5 mice were infected and pooled for reactivation analysis.

**Figure 2: Cyclin deficient virus has a similar cellular distribution to wild-type  $\gamma$ HV68 during primary infection of C57BL/6J mice.** (A) Representative gating of LANA:: $\beta$ la<sup>+</sup> splenocytes. (B) Representative gating strategy for total B cells (CD19<sup>+</sup>), germinal center B cells (CD19<sup>+</sup>, IgD<sup>-</sup>, CD38<sup>-</sup>), and activated B cells (CD19<sup>+</sup>, IgD<sup>-</sup>, CD44<sup>+</sup>). (C) and (D) representative histograms of cell surface marker expression after infection with WT. $\beta$ la or cycKO. $\beta$ la virus on total cells (dark grey WT. $\beta$ la and light grey cycKO. $\beta$ la), WT. $\beta$ la infected LANA:: $\beta$ la<sup>+</sup> cells (black), or cycKO. $\beta$ la infected LANA:: $\beta$ la<sup>+</sup> cells (red). Cells were harvested at either 8 dpi (C) or 16 dpi (D). (E) Quantification of the frequency of cells expressing cell surface markers using the gating strategy outlined in (B) with SEM shown. 8 dpi CD19, IgD and CD38 n=13. 8 DPI CD44 n=7. 16 DPI n=11. Two-tailed student t tests were performed to measure statistical significance.

**Figure 3. Disruption of the viral cyclin has no effect on the frequency of viral genome positive cells yet results in a reduced frequency of LANA:: $\beta$ la<sup>+</sup> cells.** Mice were infected via IP injection with WT. $\beta$ la or cycKO. $\beta$ la viruses and

splenocytes were harvested at 8 or 16 dpi. (A) Limiting-dilution nested PCR of viral gene ORF 50 from WT. $\beta$ la or cycKO. $\beta$ la infected splenocytes. n=4 (8 dpi) or n= 3 (16 dpi) with 3-5 mice pooled per group with SEM shown. Comparisons between the LogEC(63.2) found statistical difference between the of WT. $\beta$ la and cycKO. $\beta$ la at 8 dpi only (p=0.009). (B) Representative pseudocolor plots identifying LANA:: $\beta$ la+ splenocytes, indicated in the upper right polygon. Average frequencies of LANA:: $\beta$ la+ cells +/- SEM is indicated below the gate. 8 dpi is shown on the left, while 16 dpi is shown on the right, with WT. $\beta$ la infected mice on top and cycKO. $\beta$ la infected mice on bottom. (C) Percent of LANA:: $\beta$ la+ cells (top) and total number of LANA:: $\beta$ la+ splenocytes (bottom) from each individual mouse plotted with SEM shown after infection with WT. $\beta$ la (black) or cycKO. $\beta$ la (red) virus. (D) Graphical representation of the number of LANA:: $\beta$ la+ cells expressing cell surface markers with SEM shown after infection with WT. $\beta$ la (black) or cycK. $\beta$ la (red) virus. Cells were stained and gated as in figure 2. 8 dpi: LANA:: $\beta$ la+, CD19, IgD, and CD38 n=13 and CD44 n=7. 16 dpi n= 11. Two-tailed student t tests were performed to measure statistical significance in C and D.

**Figure 4. Disruption of the viral cyclin results in a reduced frequency of LANA:: $\beta$ la expressing cells in the peritoneum of C57BL/6J mice.** Mice were infected via IP injection with WT. $\beta$ la or cycKO. $\beta$ la viruses and peritoneal cells were harvested at 8 or 16 dpi. (A) Representative gating strategy for peritoneal cells. (B) Representative histograms of cell surface marker expression after infection with WT. $\beta$ la or cycKO. $\beta$ la virus on total cells (dark grey WT. $\beta$ la and light grey cycKO. $\beta$ la), WT. $\beta$ la  $\beta$ la+cells (black), or cycKO. $\beta$ la  $\beta$ la+ cells (red) at 8 dpi (top panel) and 16 dpi (bottom panel). (C) Representative pseudocolor plots identifying  $\beta$ la+ cells in the upper right polygon at 8 dpi (left panel) or 16 dpi (right panel) after WT. $\beta$ la (top) or cycKO. $\beta$ la (bottom) virus infection. The frequency of peritoneal cells that are  $\beta$ la+ is indicated below the gate +/- SEM. (D) Percent of cells that are  $\beta$ la+ with +/-SEM shown after infection with WT. $\beta$ la (black) or cycKO. $\beta$ la (red) virus. 8 dpi: WT. $\beta$ la n=9 and cycKO. $\beta$ la n=10. 16 dpi: n=11. Two-tailed student t tests were performed to identify statistical significance.

**Figure 5. Disruption of the viral cyclin results in a reduced frequency of LANA:: $\beta$ la expressing cells in the spleen of CD8-/- mice.** At 16 dpi, splenocytes were collected and stained for  $\beta$ -lactamase activity and cell surface markers

CD19, CD38, and IgD. CD38 and IgD samples have been previously gated on CD19+ cells. (A) Representative pseudocolor plots are shown identifying LANA:: $\beta$ la+ cells (top row). LANA:: $\beta$ la+ cells are found within the upper right polygon with the average percent of cells expressing LANA:: $\beta$ la +/- SEM indicated below the gate. Expression of CD19, IgD, and CD38 on total cells after WT. $\beta$ la virus or cycKO. $\beta$ la virus infection is shown in the indicated columns. Expression of CD19, IgD, and CD38 on LANA:: $\beta$ la+ cells is shown in the indicated columns. The average percent of cells that fall within each gate is indicated +/- SEM. (B) Graphical representation of the percent of cells that are LANA:: $\beta$ la+ after WT. $\beta$ la (black) or cycKO. $\beta$ la (red) infection with SEM. (C) Graphed are the average percent of cells that are CD19+ and the percent of CD19+ cells that are IgD+/CD38-, IgD+/CD38+, IgD-/CD38+, and IgD-/CD38- after WT. $\beta$ la (black) or cycKO. $\beta$ la (red) infection. Total cells are graphed on the top while LANA:: $\beta$ la+ gated cells are shown on the bottom, both with SEM plotted. Two experiments were performed with 3-4 WT. $\beta$ la and cycKO. $\beta$ la infected mice per experiment. WT. $\beta$ la: n=7; cycKO. $\beta$ la: n=6

**Figure 6. Disruption of the viral cyclin results in a reduced frequency of LANA:: $\beta$ la expressing cells in the peritoneum of CD8-/- mice.** CD8-/- mice were inoculated with WT. $\beta$ la virus or cycKO. $\beta$ la virus via IP injection. At 16 dpi, peritoneal cells were collected and stained for  $\beta$ -lactamase activity and cell surface markers CD19, B220, and CD5. (A) Representative pseudocolor plots are shown identifying LANA:: $\beta$ la+ cells (top row). LANA:: $\beta$ la+ cells are found within the upper right polygon with the average percent of cells expressing LANA:: $\beta$ la +/- SEM indicated below the gate. Expression of CD19, B220, and CD5 on total cells after WT. $\beta$ la virus or cycKO. $\beta$ la virus infection is shown in the indicated columns. Expression of CD19, B220, and CD5 on LANA:: $\beta$ la+ cells is shown in the indicated columns. The average percent of cells that fall within each gate is indicated +/- SEM. (B) Graphical representation of the percent of cells that are LANA:: $\beta$ la+ after WT. $\beta$ la (black) or cycKO. $\beta$ la (red) infection with SEM. (C) Graphed are the average percent of cells that are CD19+, B1-a (CD5+), B1-b (B220 intermediate), and B2 (B220 high) after WT. $\beta$ la (black) or cycKO. $\beta$ la (red) infection. Total cells are graphed on the top while LANA:: $\beta$ la+ gated cells are shown on the bottom, both with SEM plotted. Two experiments were performed with 3-4 WT. $\beta$ la and cycKO. $\beta$ la infected mice per experiment. WT. $\beta$ la: n=6 cycKO. $\beta$ la: n=7. (D) Relative expression of  $\beta$ -lactamase (top) and LANA

(bottom). RNA was isolated from infected peritoneal cells and subjected to quantitative RT-PCR analysis using primers directed against  $\beta$ -lactamase (top) and LANA (bottom). mRNA expression levels depicted were normalized to 18S levels, with differences between WT.  $\beta$ la and cycKO. $\beta$ la as noted.

**Figure 7. The viral cyclin is dispensable for reactivation in latently infected cells that express LANA:: $\beta$ la. (A)**

Experiment schematic. CD8<sup>-/-</sup> mice were infected via IP injection with WT. $\beta$ la or cycKO. $\beta$ la viruses and peritoneal cells were harvested at 16 dpi. Cells were stained for  $\beta$ -lactamase activity and LANA:: $\beta$ la<sup>+</sup> cells were sorted by FACS. (B) Gating strategy of LANA:: $\beta$ la sort (left) and purity of post-sort WT. $\beta$ la infected LANA:: $\beta$ la<sup>+</sup> cells (right). LANA:: $\beta$ la<sup>+</sup> cells are located in the upper right polygon and LANA:: $\beta$ la<sup>-</sup> cells are located in the upper left polygon. The percent of events within each gate is indicated below the gate. (C) WT. $\beta$ la (black) and cycKO. $\beta$ la (red) infected pre-sorted (left), LANA:: $\beta$ la<sup>-</sup> (middle), and LANA:: $\beta$ la<sup>+</sup> (right) cells were subjected to limiting-dilution reactivation analysis. Reactivation was measured 21 days after plating sorted and pre-sorted cells on permissive MEFs. Linear regression with comparison of the LogEC(63.2) found that there was a statistical difference in reactivation between LANA:: $\beta$ la<sup>+</sup> WT. $\beta$ la and cycKO. $\beta$ la infected cells and pre-sorted WT. $\beta$ la and cycKO. $\beta$ la infected cells ( $p < 0.0001$ ).  $n = 2$  independent experiments with a total of 15 WT. $\beta$ la infected mice and 30 cycKO. $\beta$ la infected mice. The table below lists the number of cells plated to reach CPE in 63.2% (the dotted line) of the wells plated for reactivation, corresponding to the number of cell required to find at least 1 reactivating cell.

**Figure 8. The viral cyclin drives reactivation through increasing the pool of LANA expressing, reactivation-competent, infected cells.** Wild-type  $\gamma$ HV68 infection results in establishment of latency (depicted by nuclear viral episomes). At least two distinct populations of latently infected cells arise, cells expressing viral LANA (gray) and those lacking detectable LANA expression (white). The LANA expressing cells are permissive to reactivation and will readily reactivate when triggered. Latent cells lacking LANA are incapable of reactivation, and instead remain dormant in latency. Infection with a viral cyclin-deficient  $\gamma$ HV68 virus also results in establishment of latency, with equivalent numbers to wild-type infection. However, without the viral cyclin, latency is skewed to reactivation incompetent, LANA negative cells. The cyclin-deficient infected cells which do express LANA are still able to

reactivate, as efficiently as wild-type, but there are diminished numbers of these cells ultimately leading to the reactivation defect.

Figure 1: Characterization of the cyclin-deficient virus expressing a LANA  $\beta$ -lactamase gene fusion.

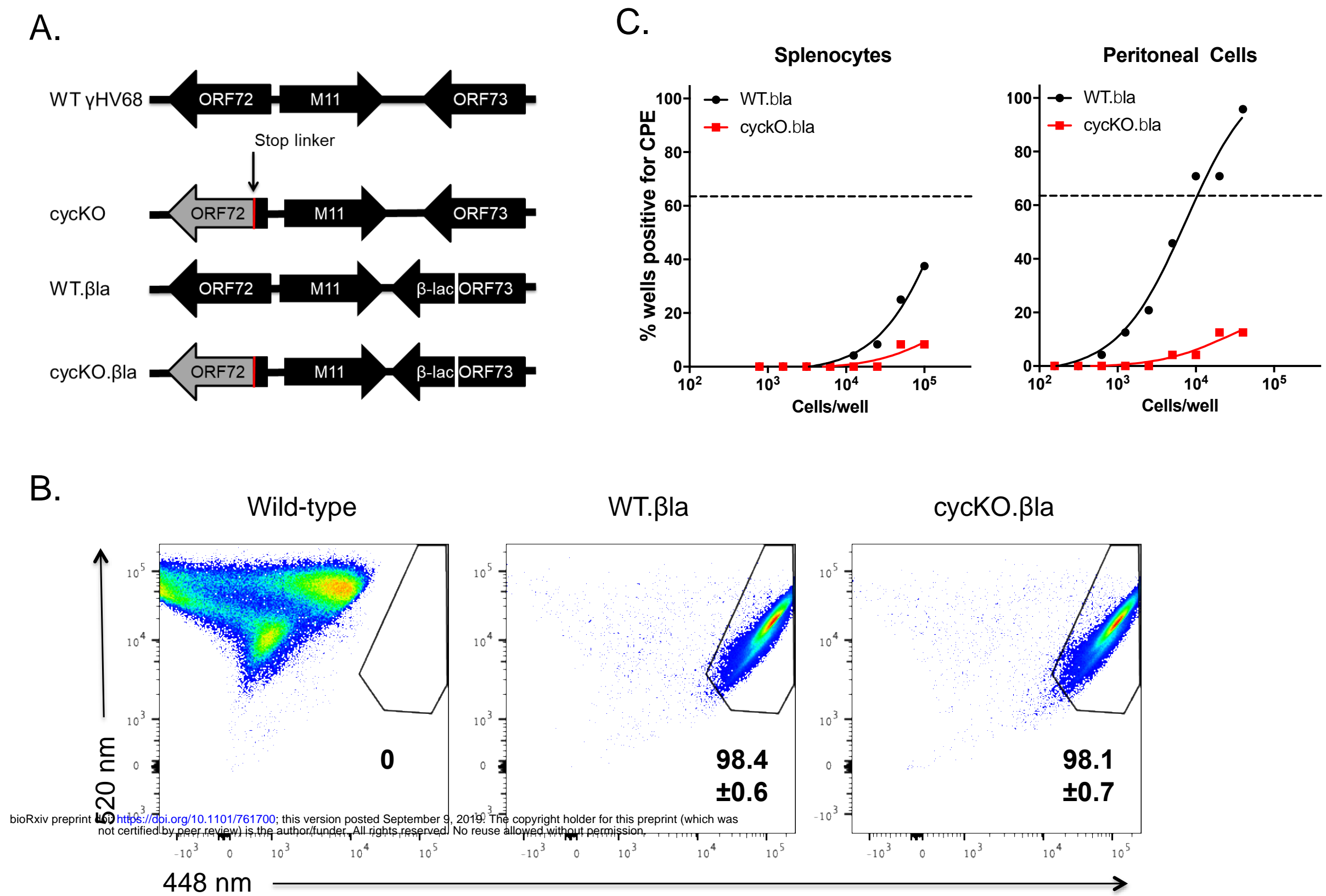


# Figure 2: Cyclin deficient virus has a similar cellular distribution to wild-type $\gamma$ HV68 during primary infection of C57BL/6J mice

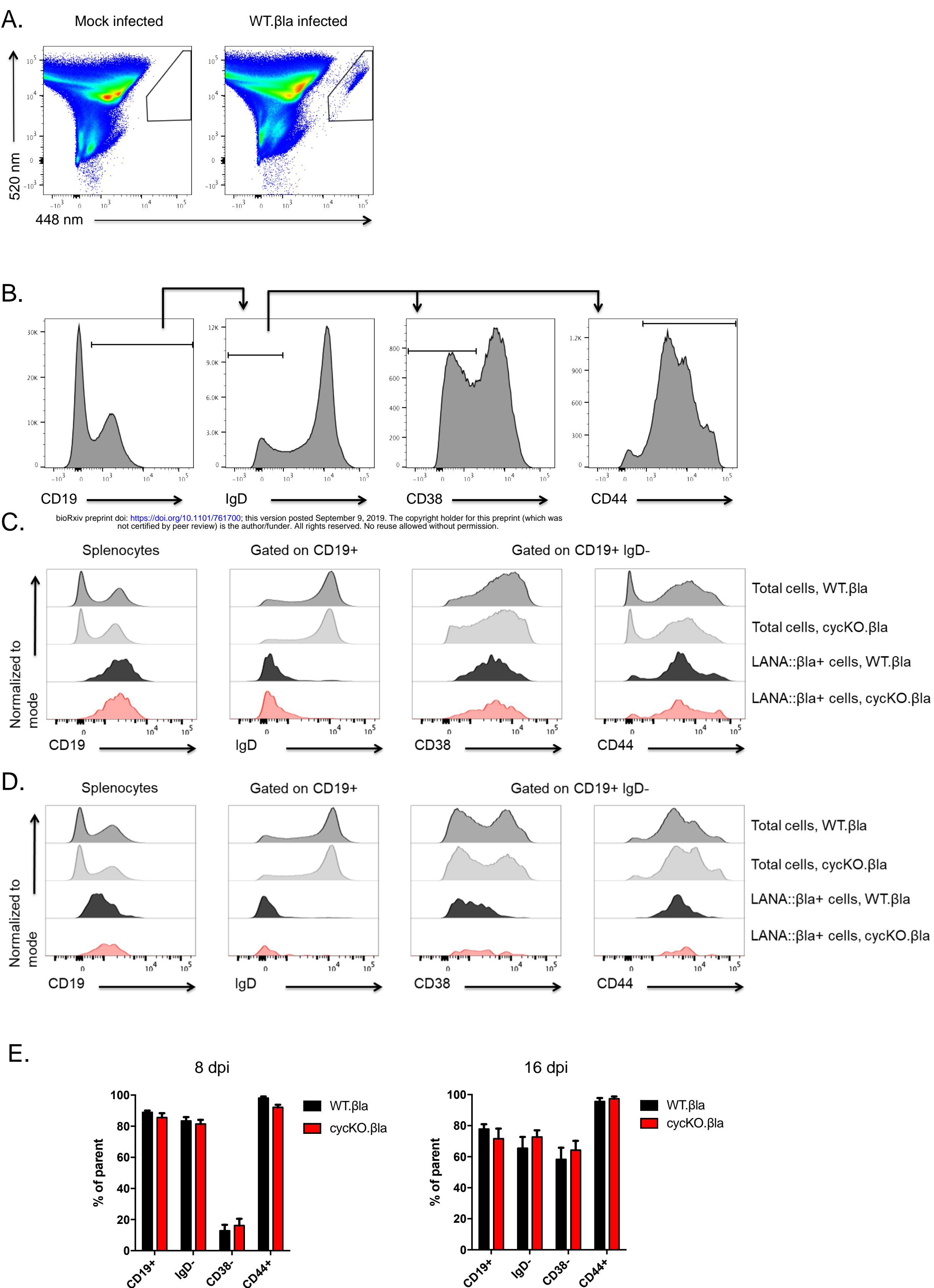
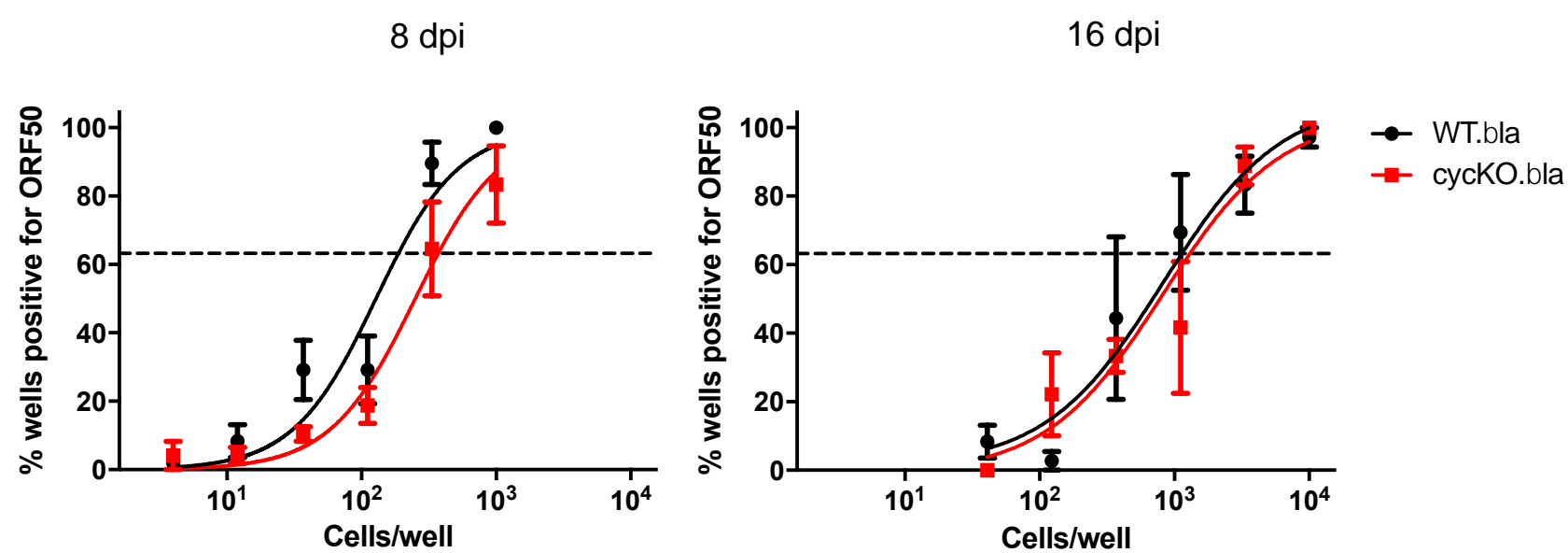
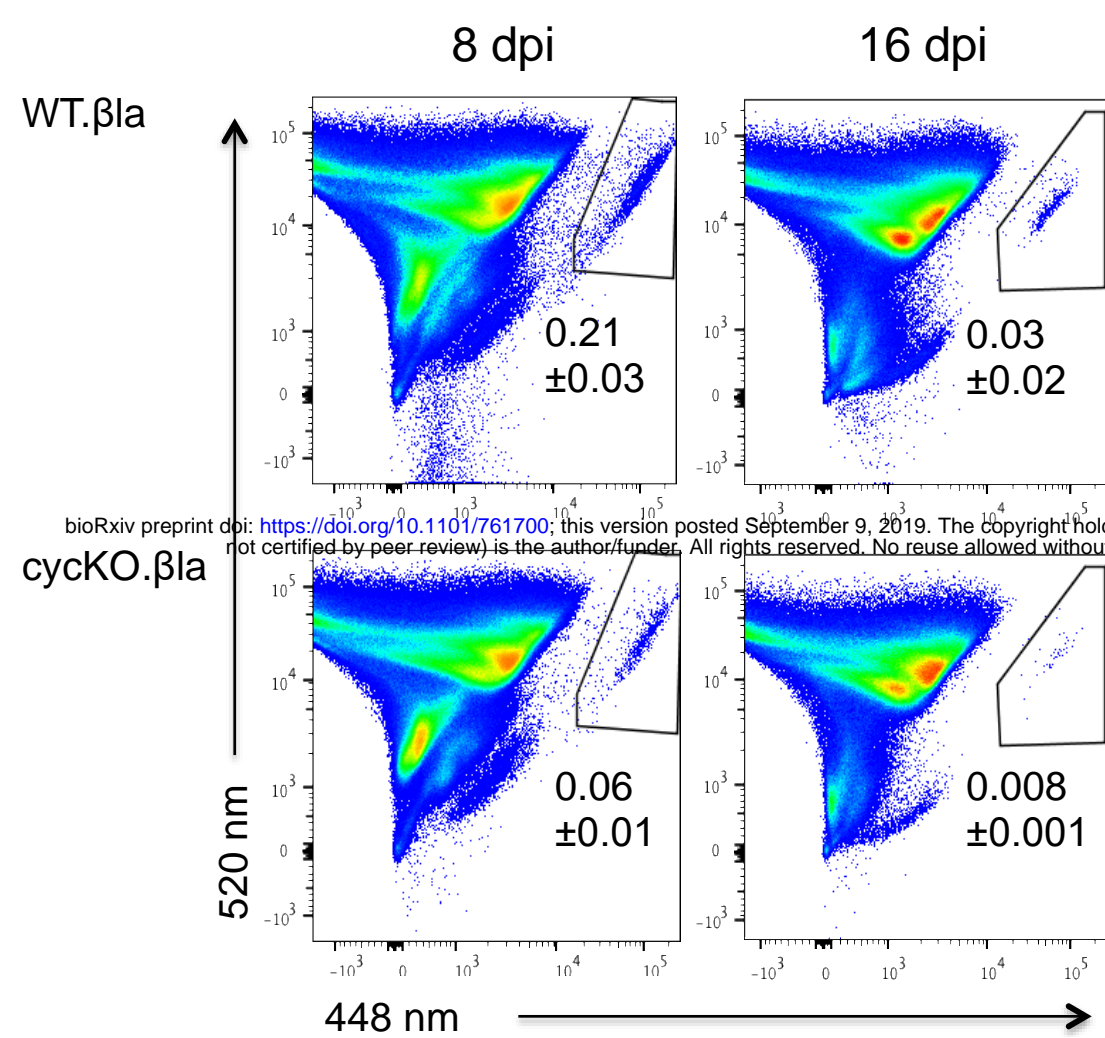


Figure 3: Disruption of the viral cyclin has no effect on the frequency of viral genome positive cells yet results in a reduced frequency of LANA::βla+ cells

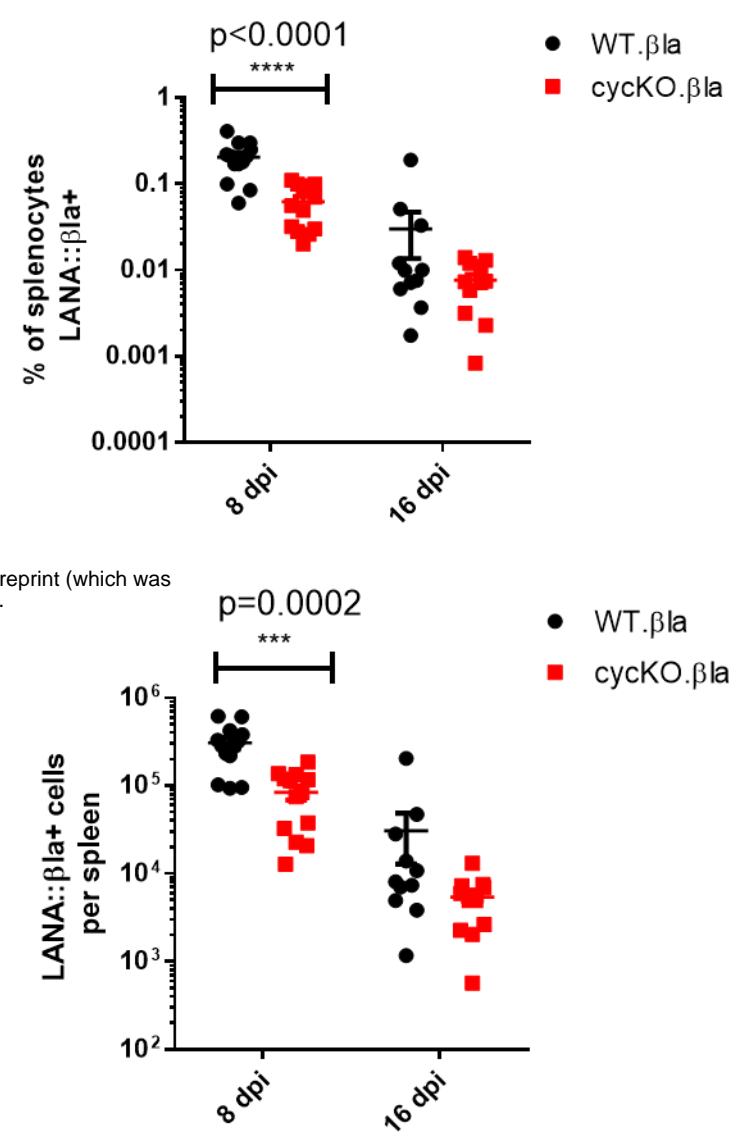
A.



B.



C.



D.

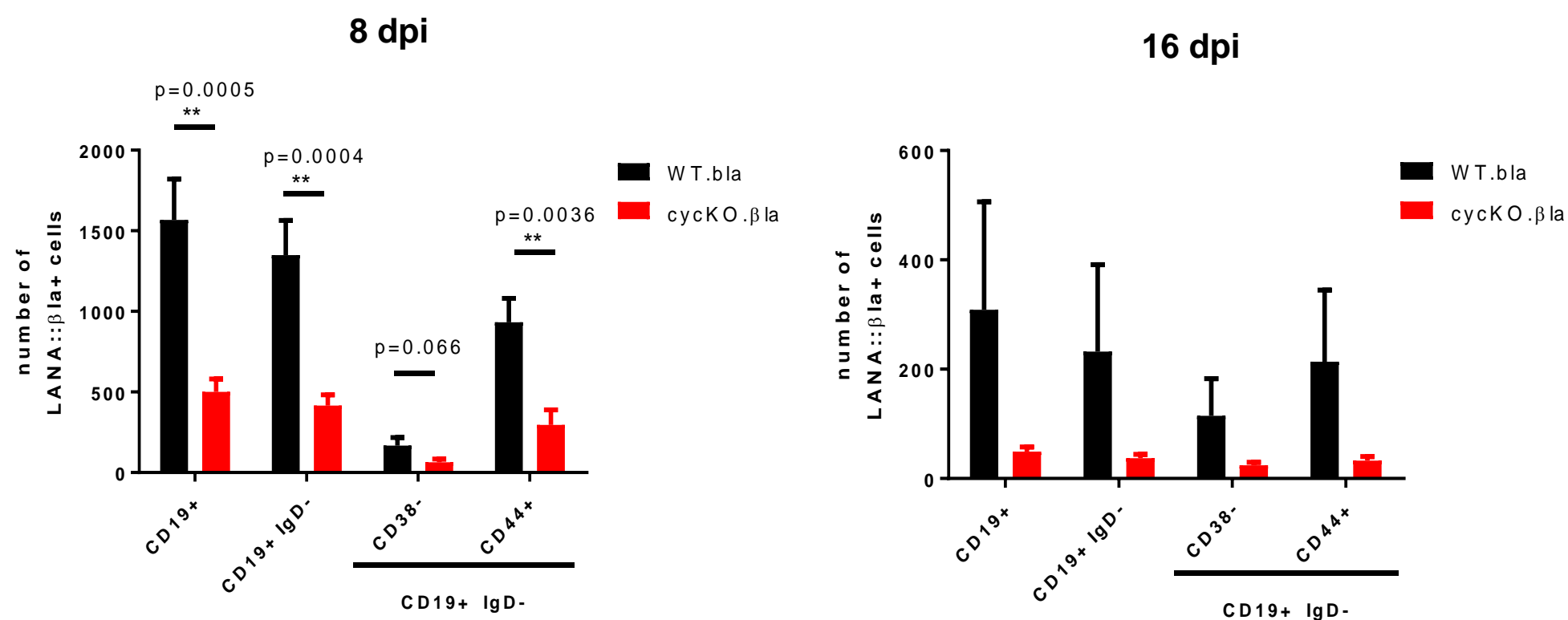




# Figure 4: Disruption of the viral cyclin results in a reduced frequency of LANA::βla expressing cells in the peritoneum of C57BL/6J mice

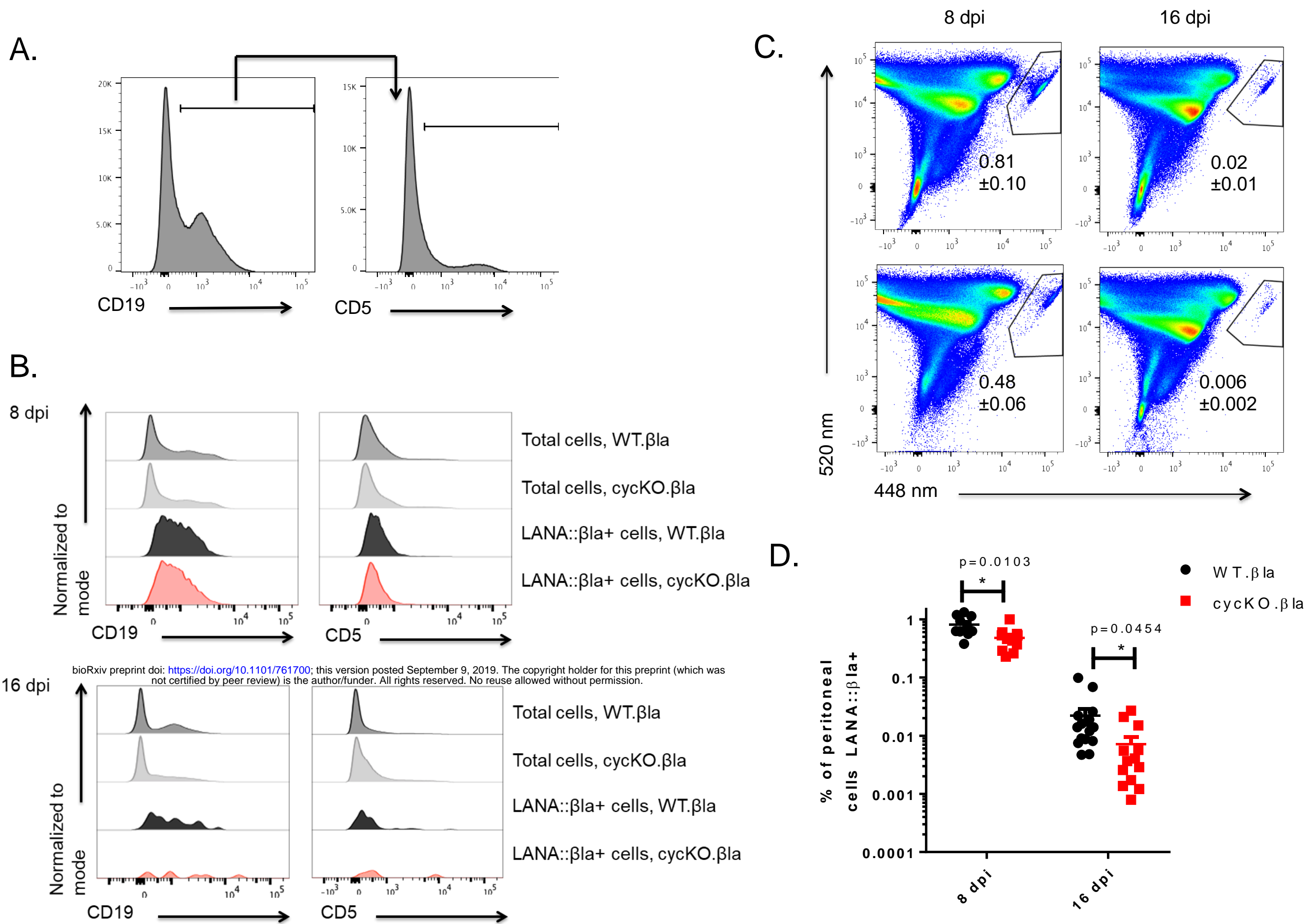


Figure 5: Disruption of the viral cyclin results in a reduced frequency of LANA::βla expressing cells in the spleen of CD8<sup>-/-</sup> mice

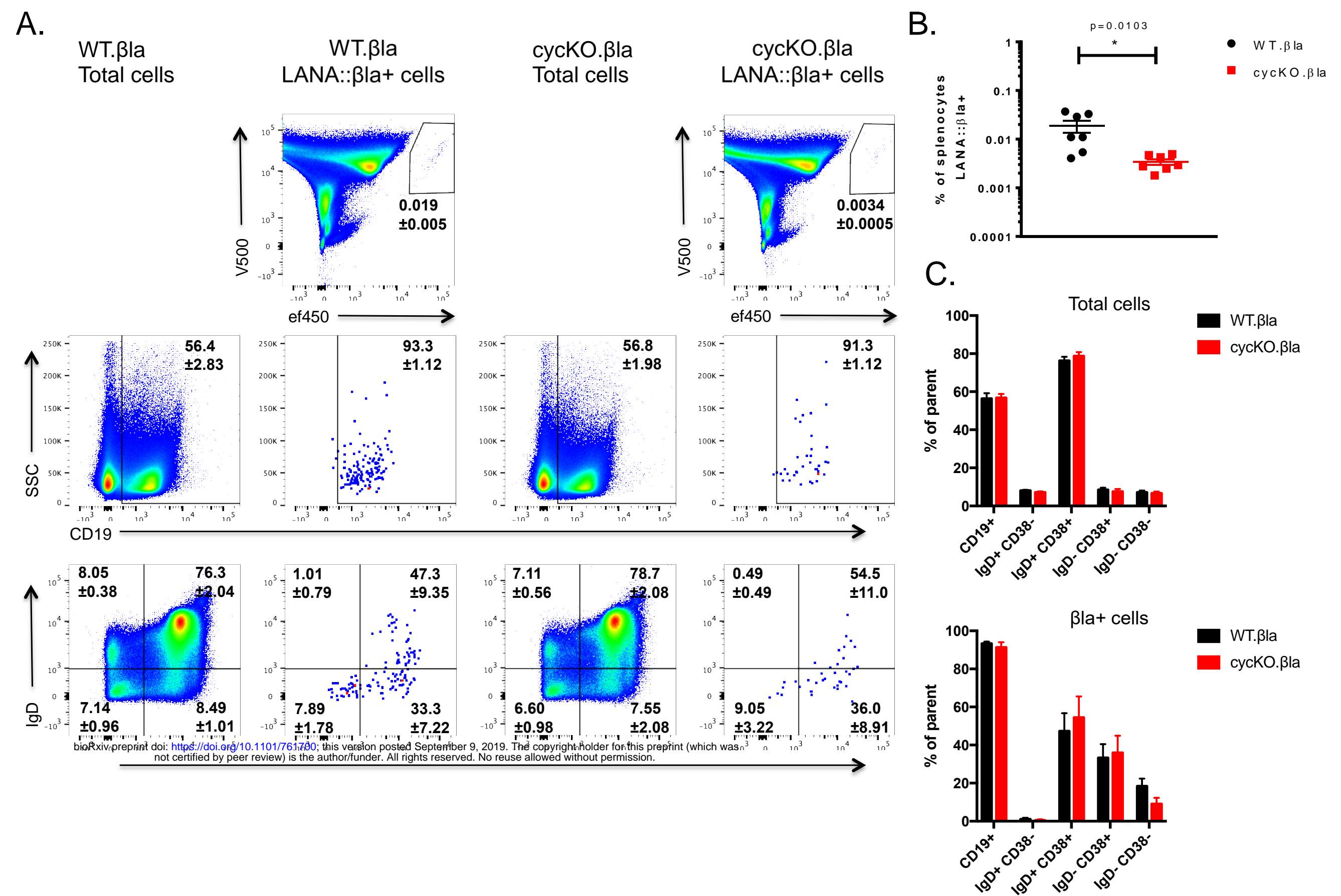
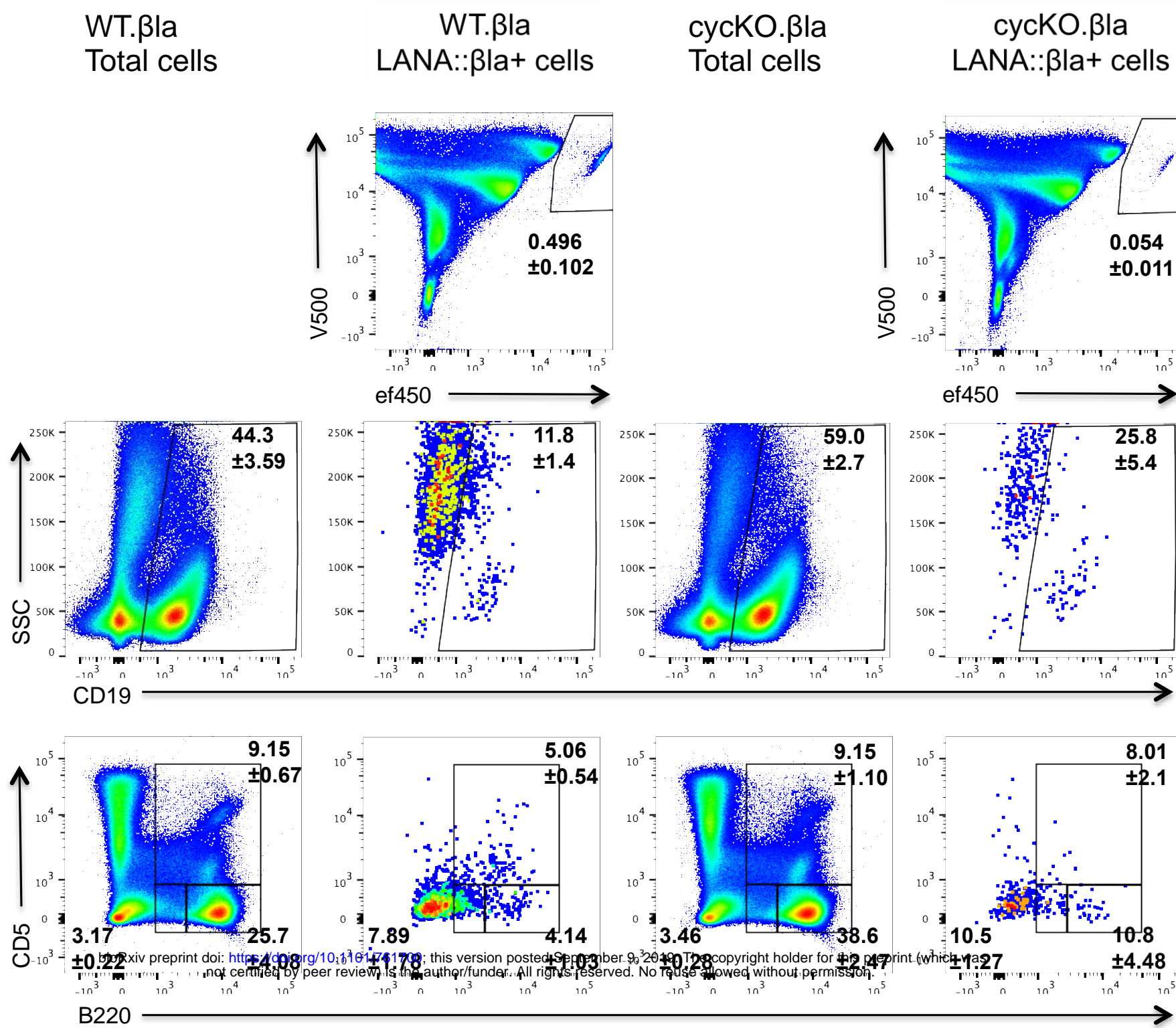
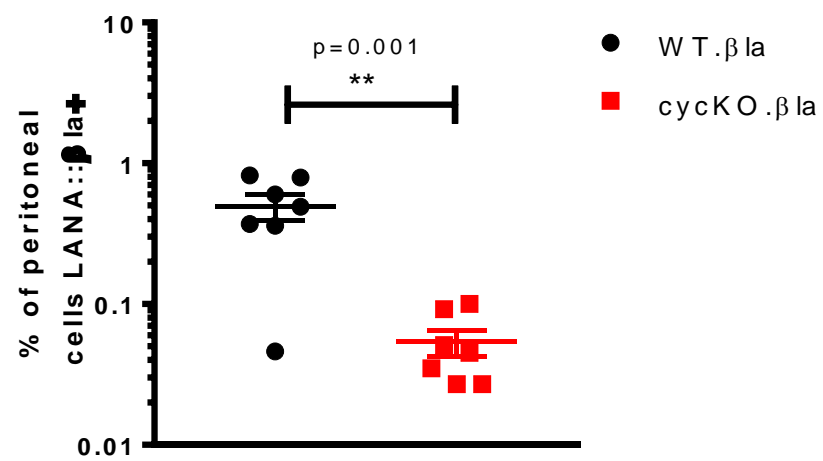


Figure 6: Disruption of the viral cyclin results in a reduced frequency of LANA::βla expressing cells in the peritoneum of CD8<sup>-/-</sup> mice.

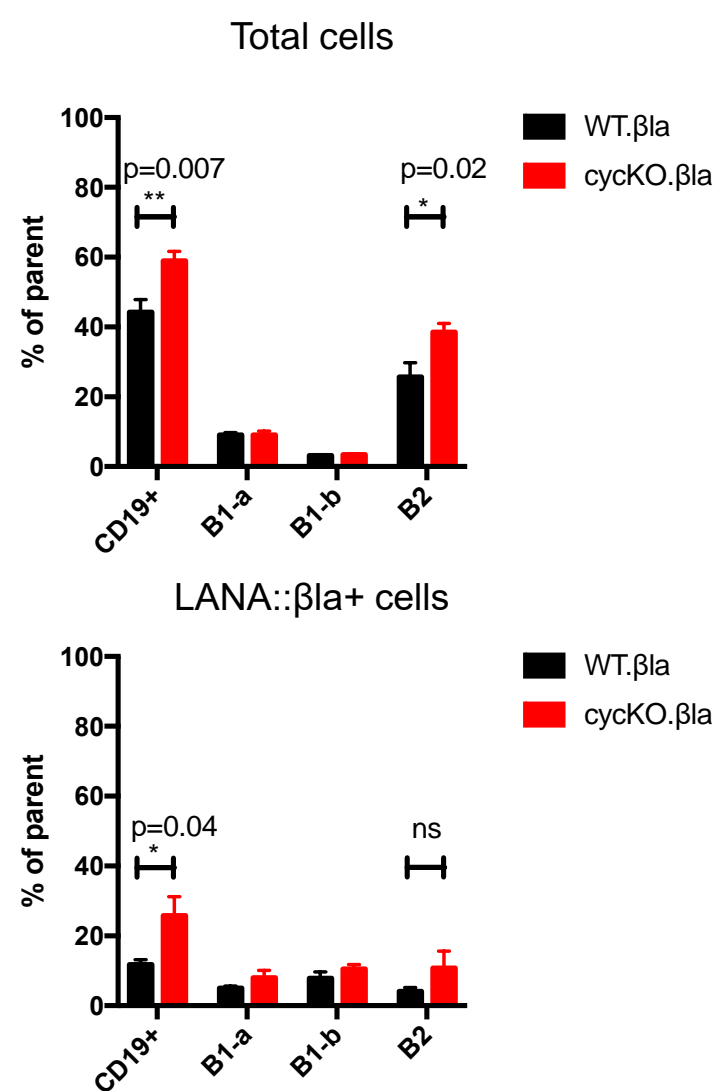
A.



B.



C.



D.

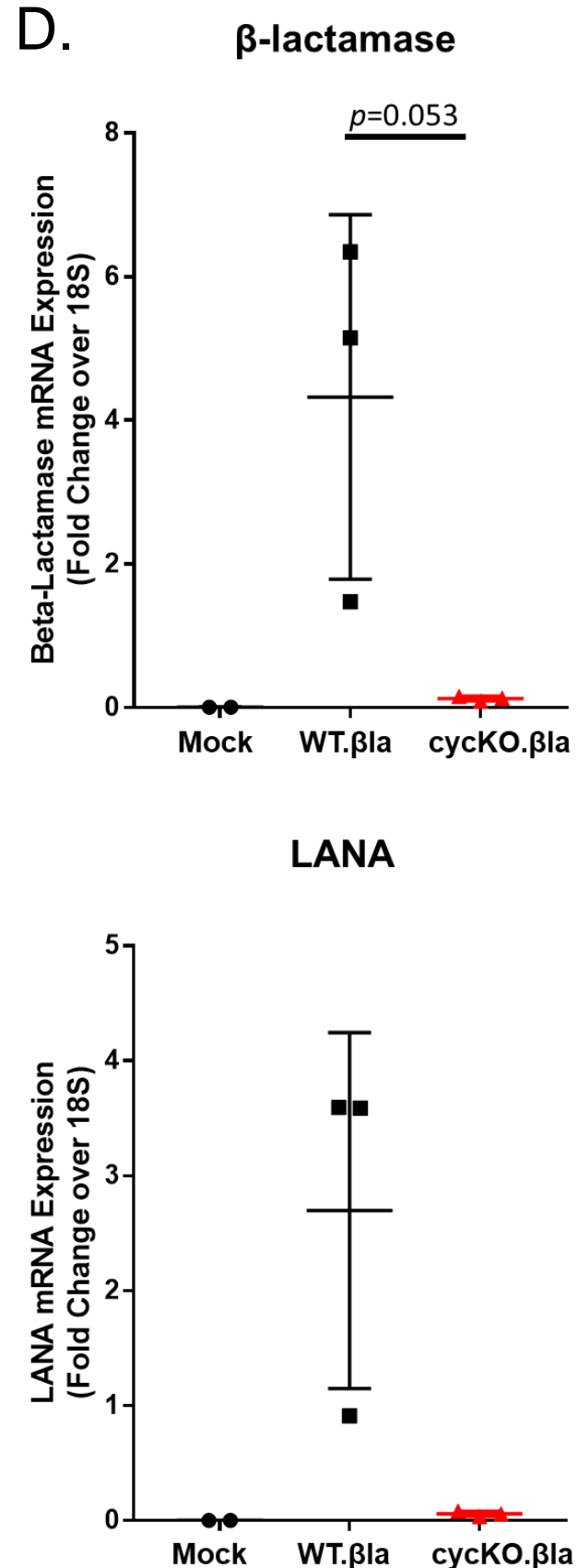
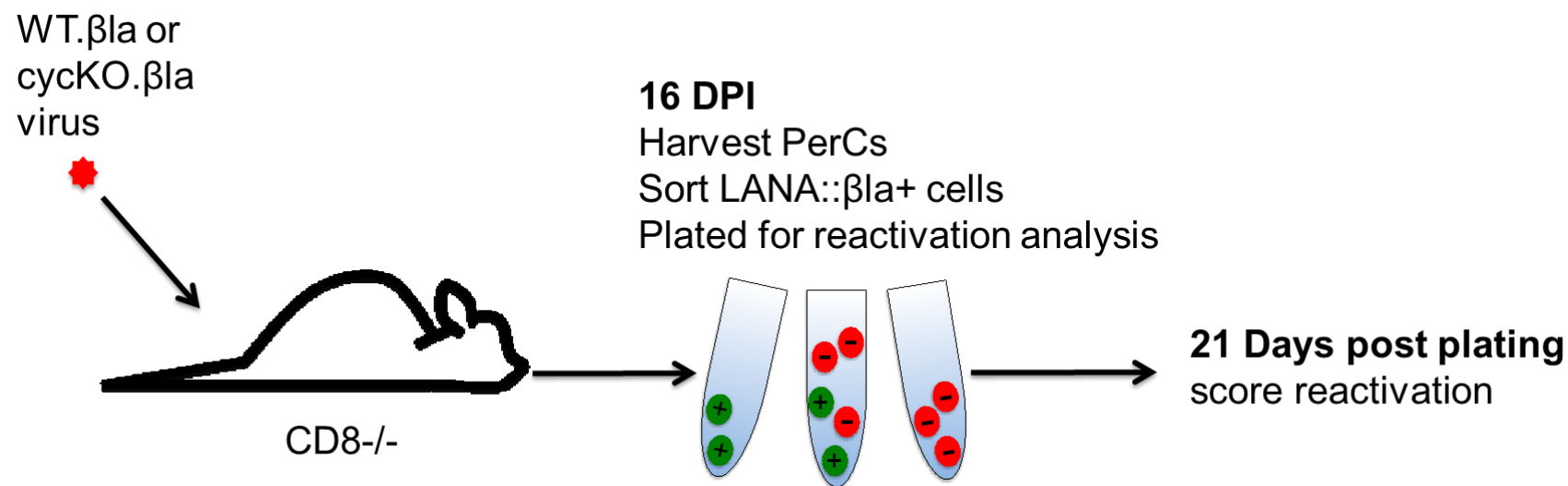
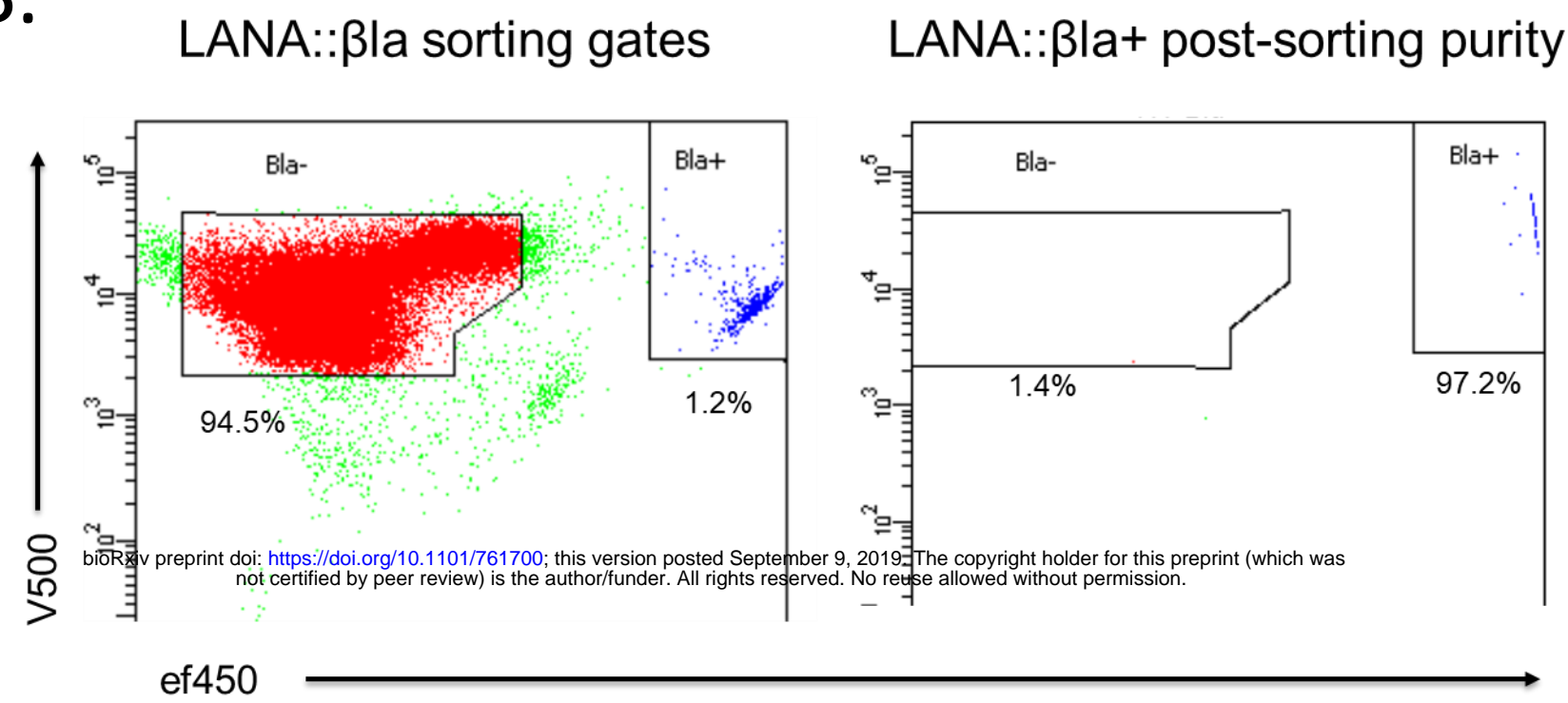


# Figure 7: The viral cyclin is dispensable for reactivation in latently infected cells that express LANA::βla

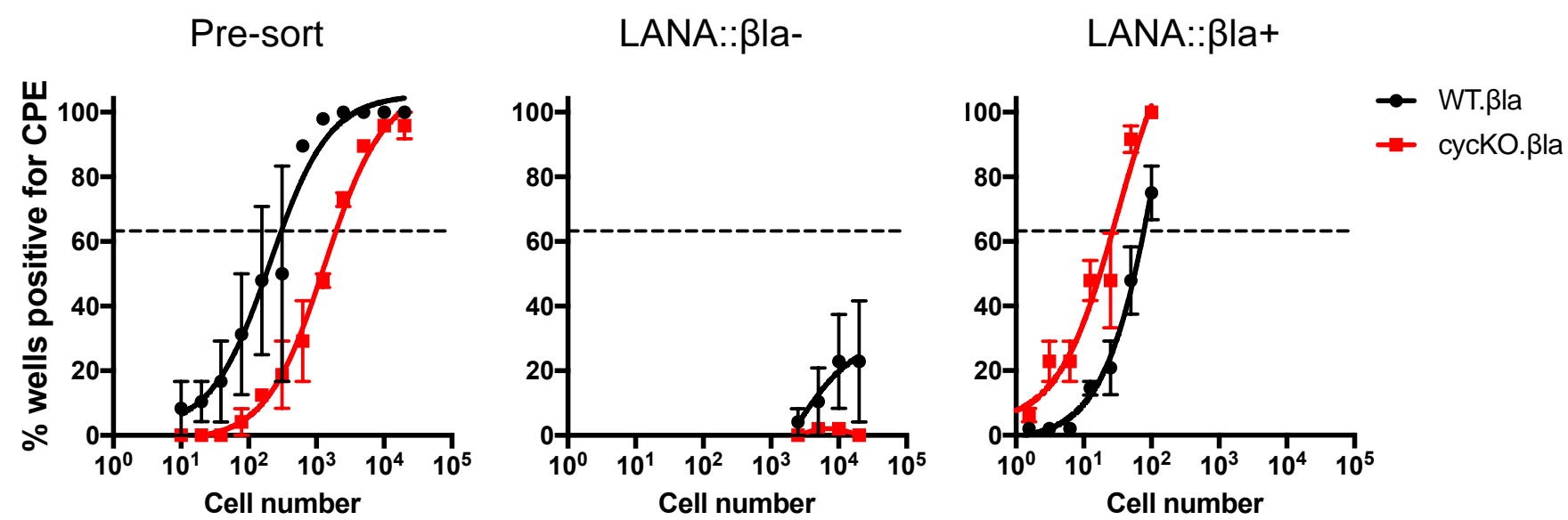
A.



B.



C.



Virus	Sort-status	1/x cells reactivating	P value
WT.βla	pre-sort	281	<0.0001
cycKO.βla	pre-sort	1811	
WT.βla	LANA::βla+	73	<0.001
cycKO.βla	LANA::βla+	24	

Figure 8. The viral cyclin drives reactivation through increasing the pool of LANA expressing, reactivation-competent, infected cells.

